

SAMPLEIV [EASA.2020.FC05]

[DELIVERABLE 5: DATA REPORT]

Small and non-regulated engine emission tests

Disclaimer



Funded by the European Union. Views and opinions expressed are however those of the author(s) only and do not necessarily reflect those of the European Union or the European Union Aviation Safety Agency (EASA). Neither the European Union nor EASA can be held responsible for them.

This deliverable has been carried out for EASA by an external organisation and expresses the opinion of the organisation undertaking this deliverable. It is provided for information purposes. Consequently, it should not be relied upon as a statement, as any form of warranty, representation, undertaking, contractual, or other commitment binding in law upon the EASA.

Ownership of all copyright and other intellectual property rights in this material including any documentation, data and technical information, remains vested to the European Union Aviation Safety Agency. All logo, copyrights, trademarks, and registered trademarks that may be contained within are the property of their respective owners. For any use or reproduction of photos or other material that is not under the copyright of EASA, permission must be sought directly from the copyright holders.

Reproduction of this deliverable, in whole or in part, is permitted under the condition that the full body of this Disclaimer remains clearly and visibly affixed at all times with such reproduced part.

| | |
|--------------------------------------|--|
| DELIVERABLE NUMBER AND TITLE: | SAMPLEIV, D5 |
| CONTRACT NUMBER: | EASA.2020.FC05 |
| CONTRACTOR / AUTHOR: | Dr's E. Durand (CU), A Crayford (CU), M. Johnson (RR), P. Williams (UoM), Jesus Sanchez Valdepeñas Garcia Moreno (INTA), Rocio Gallardo Martinez (INTA), Paul Williams (UoM) & Lukas Durdina |
| IPR OWNER: | European Union Aviation Safety Agency |
| DISTRIBUTION: | Public |

DATE: March 2025

EXECUTIVE SUMMARY

Gas turbine engines with a rated thrust of <26.7 kN, commonly found in business jets, light regional aircraft, and military applications, are currently regulated only for visible smoke, with no specific controls on gaseous or non-volatile particulate matter (nvPM) emissions. While their overall contribution to global aviation is relatively modest, the use of these non-regulated engines is increasing, and their emissions remain largely unquantified.

This report presents newly acquired gaseous, nvPM and smoke engine-exit emissions data for small engines that do not have nvPM data available in the ICAO databank (Honeywell ALF 502-R5 and 507-1H) in addition to nvPM data from a non-regulated turboprop engine (Pratt & Whitney PW127G). Descriptions of the specific experimental setups, including details of the bespoke designed exhaust probes, sampling and measurement systems, and data analysis methods are provided for each of the test campaigns.

Emissions data for the three aforementioned engines, in addition to nvPM data from a further three non-regulated engines in the 16-22 kN thrust range, which was acquired in previous test campaigns by the Swiss State-of-the-art aircraft engine emissions measurement system (SMARTEMIS) nvPM system are presented. This data is processed to afford comparison to the maximum nvPM mass and number regulatory limits set by ICAO for the reference LTO cycle (CAEP/11), and the maximum nvPM mass concentration (CAEP/10), as defined for regulated engines.

The findings of this analysis indicate that lower thrust and non-regulated engines produce nvPM and gaseous emissions comparable to those of regulated engines, with emission levels generally well below the ICAO regulatory thresholds for in-production engines. However, nvPM emissions varied significantly among the tested engines. The ALF 502 and LF 507 emitted relatively low concentrations of small nvPM, whereas the tested turboprop (PW127G) witnessed higher concentrations of larger PM emissions across the entire power range.

During the ALF 502/ LF507 testing a novel, simplified sampling and measurement approach was developed and validated against the European nvPM reference sampling and measurement system. This novel approach was then deployed for the PW127G test. This method utilised a Dekati eDiluter™ Pro, which facilitated CO₂ and PM measurements at either the first (5:1–15:1 dilution) or second (25:1–225:1 dilution) controllable dilution stages. This sampling setup offers a practical and simplified means of acquiring nvPM emissions data.

In addition to the emissions data presented here for standard fossil-based Jet A fuel, the same experimental set-up was used to evaluate the impact of fuel composition on observed nvPM emissions during small engine testing. Further details of this fuel impact can be found in the SAMPLE IV Deliverable 7 report, with the data also used to further assess methodologies for estimating nvPM emissions from smoke number as discussed in the SAMPLE IV Deliverable 6 report.

TABLE OF CONTENTS

| | |
|--|----|
| EXECUTIVE SUMMARY..... | 3 |
| TABLE OF CONTENTS | 4 |
| LIST OF FIGURES | 5 |
| LIST OF TABLES | 6 |
| LIST OF ABBREVIATIONS..... | 7 |
| 1. Introduction..... | 8 |
| 2. nvPM Emissions Testing of Small Gas Turbine Engines..... | 8 |
| 2.1. Experimental methods | 9 |
| 2.2. LF507-1H and ALF502-R5 Emissions Results | 16 |
| 3. Emissions Testing of Non-regulated Turboprop engine..... | 21 |
| 3.1. Experimental methods | 21 |
| 3.2. Emissions Results..... | 28 |
| 4. Summary of nvPM emissions from small and non-regulated engines..... | 34 |
| 4.1. ICAO nvPM regulatory levels | 34 |
| 4.2. N/M Vs GMD | 35 |
| ACKNOWLEDGEMENTS | 36 |
| REFERENCES | 37 |
| APPENDIX | 39 |
| AVL MSS calibration certificate | 39 |
| AVL APC calibration certificate (VPR+CPC) | 40 |
| Gas analysers' linearity certificates..... | 43 |

LIST OF FIGURES

| | |
|---|----|
| Figure 1: photographs of test engine on the CFS aero Hawarden test stand (left), sampling probe and near-field measurement cabinet (middle), and main measurement cabin (right) | 9 |
| Figure 2: Diagram of the top-level assembly (left) and support arrangements (right) used on CFS Aero test bed | 9 |
| Figure 3: schematic and spatial locations of the sampling probe with the equal area sampling points (front-view left) and sample intake (side-view right) | 10 |
| Figure 4: Simplified diagram of the full sampling and measurement system (note full details of the novel experiments setup is available in the SAMPLE IV Deliverable 3 report ⁷) | 11 |
| Figure 5: Number concentration comparison between additional and EUR nvPM reference CPC behind the VPR of the EUR APC during a full engine curve when sampling the ALF502 | 12 |
| Figure 6: Measured EI NO _x during LF507 ‘shakedown’ testing highlighting equivalent T30 points of LTO reported values (datapoints intersecting with black dashed lines) | 12 |
| Figure 7: Measured EI THC during LF507 ‘shakedown’ testing highlighting equivalent T30 points of LTO reported values (datapoints intersecting with black dashed lines) – 85% and 100% LTO points have EI THC ~ 0 g/kg | 13 |
| Figure 8: Measured EI CO during LF507 ‘shakedown’ testing highlighting equivalent T30 points of LTO reported values (datapoints intersecting with black dashed lines) – 85% and 100% LTO points have EI CO ~ 0 g/kg | 13 |
| Figure 9: Measured (uncorrected) PM number concentrations (blue) and particle sizes (red) during LF507 ‘shakedown’ testing | 14 |
| Figure 10: Engine T30 Vs Thrust for the LF507 (left) and ALF502 (right engines) | 14 |
| Figure 11: Regulatory HC (left) CO (middle) and NO _x (right) emission indices against thrust for different fuels on the LF507 and ALF502 | 17 |
| Figure 12: Corrected raw CO ₂ emissions against thrust for different fuels on the LF507 and ALF502 | 18 |
| Figure 13: Measured Smoke number against thrust for the LF507 and ALF502 engines | 18 |
| Figure 14: nvPM EI number (left) and EI mass (right) against thrust for the LF507 and ALF502 | 19 |
| Figure 15: Loss-corrected nvPM EI number (left) and EI mass (right) emissions against thrust for the LF507 and ALF502 engines | 20 |
| Figure 16: Engine exit Geometric Mean Diameter (GMD) derived from a Grimm SMPS+C 5420 against thrust for the LF507 and ALF502 engines | 20 |
| Figure 17: Diagram of the dedicated INTA probe used during PW127G emissions testing | 21 |
| Figure 18: Diagram (left) and picture (right) of the dedicated INTAO probe orientation towards the engine exhaust | 22 |
| Figure 19 Diagram of the dedicated INTA probe length (left) and picture of probe mounted on the structure (right) | 22 |
| Figure 20: Pictures of the INTA dedicated probe and structure with concrete ballast used to weight down the structure | 23 |
| Figure 21: Diagram of the experimental set up used to measure the emissions of the PW127G | 24 |
| Figure 22: Pictures of a) Instruments located in the death box, b) Instruments located in the cabin, c) Heated lines | 24 |
| Figure 23: Probe inlet temperature representing engine-exhaust temperature plotted against engine shaft power for three up and down curves | 26 |
| Figure 24: Timeseries of the PW127G shaft power on 18 th October 2024 | 27 |

| | |
|--|----|
| Figure 25: CO ₂ measured on the raw probe (left) and diluted probe behind the 1 st stage of the eDiluter pro (right) against engine shaft power | 29 |
| Figure 26: Fuel flowrate (left) and measured DF ₁ (right) against engine shaft power..... | 29 |
| Figure 27: PM number measured by the Grimm 5420 CPC behind the eDiluter™ 2 nd stage plotted against the total number from the TSI SMPS behind the eDiluter™ 1 st stage while sampling PW127G exhaust | 30 |
| Figure 28: Geometric Mean Diameter (left) and Particle Size distribution (right) measured by the SMPS at different engine power conditions while sampling PW127G exhaust..... | 30 |
| Figure 29: total PM EI number derived from the SMPS (left) and from the CPC (right) | 31 |
| Figure 30: PM EI mass derived from the SMPS | 31 |
| Figure 31: nvPM EI number (left) and total PM to nvPM ratio (right) against shaft power | 32 |
| Figure 32: Timeseries showing the shaft power (orange – left y-axis) and total and non-volatile PM CPCs measurements (blue and grey – right y-axis)..... | 33 |
| Figure 33: nvPM mass (left) and number (right) emitted during the reference LTO for various small and non-regulated engines..... | 35 |
| Figure 34: Maximum nvPM mass (measured x k _{thermo} x DF ₁) for various small and non-regulated engines | 35 |
| Figure 35: Engine exit plane nvPM GMD as a function of the ratio of regulatory system loss (SL) corrected nvPM number to mass (N/M) with Durdina et al. fit [13] (dashed lines represent 95% confidence intervals) .. | 36 |

LIST OF TABLES

| | |
|---|----|
| Table 1: Test points achieved during LF507 and ALF502 engines emission testing with their corresponding engine power | 15 |
| Table 2: Summary of fuel properties during LF507 and ALF502 engine emission testing | 15 |
| Table 3: Regulatory gaseous and smoke emissions for the LF507 and ALF502 copied from the ICAO emissions databank (V30)..... | 17 |
| Table 4: Regulatory-equivalent nvPM EI emissions for the ALF 507 and 502 | 19 |
| Table 5: Dimensions and materials of the sample lines installed | 25 |
| Table 6: Flowrates and properties of the instruments used in the experimental campaign (flowrate was measured using a TSI 4140 flowmeter) | 26 |

LIST OF ABBREVIATIONS

| | |
|----------|---|
| APC | – AVL Particle Counter |
| ASTM | - American Society for Testing and Materials |
| CAEP | - Committee on Aviation Environmental Protection |
| CPC | – Condensation Particle Counter |
| CS | – Catalytic Stripper |
| CU | – Cardiff University |
| DF | – Dilution Factor |
| DMA | – Differential Mobility Analyzer |
| DMS | – Differential Mobility Spectrometer (Combustion) |
| EED | – Engine Emission Databank (ICAO) |
| EI | – Emission Index |
| EUR | - European |
| GMD | – Geometric Mean Diameter |
| GSD | – Geometric Standard Deviation |
| ICAO | – International Civil Aviation Organization |
| INTA | – Instituto Nacional De Técnica Aeroespacial “Esteban Terradas” |
| k_{SL} | – Size-dependent system loss correction factor |
| LII | – Laser Induced Incandescence |
| LTO | – Landing Take-Off cycle |
| MSS | – Micro Soot Sensor (AVL) |
| NDIR | – Non-Dispersive InfraRed |
| nvPM | – Non-Volatile Particulate Matter |
| PM | – Particulate Matter |
| PSD | – Particle Size Distribution |
| RR | – Rolls-Royce |
| SAF | – Sustainable Aviation Fuel |
| SMPS | – Scanning Mobility Particle Sizer |
| SN | – Smoke Number |
| STP | – Standard Temperature and Pressure |
| TC | – Thermocouple |
| THC | – Total unburnt Hydrocarbons |
| VPR | – Volatile Particle Remover |

1. Introduction

In light of the existing smoke number regulation not assuring the control of number concentrations of particulate matter (PM) emitted from large civil-aviation engines, as of CAEP/10 a new non-volatile PM (nvPM) mass regulatory limit for gas turbine engines with a rated thrust of >26.7 kN was adopted by ICAO in 2020. This regulatory nvPM limit was then further enhanced with the addition of an nvPM number standard, which was adopted in January 2023 (CAEP/11).

However, as further discussed in the SAMPLE IV Deliverable 4 report¹, at smaller EU airports there can often be significant relative utilisation (in terms of number of flights) of non-regulated engines (piston, Turboprop and turbofan <26.7 kN), with the analysis suggesting that this contribution is circa 34% of flights at Trondheim airport. Non-regulated engines are commonly found in business jets, light regional aircraft, and military applications, and are currently only regulated for visible smoke, with no specific controls on gaseous or nvPM emissions. While their overall contribution to global aviation emissions is relatively modest, the use of these non-regulated engines is currently increasing, with their exact nvPM emissions remaining largely unquantified or predicted using data derived using non-standard measurement practices or from correlations to measured smoke number².

To increase understanding of real-world emissions from engines which are not detailed for nvPM in the ICAO Engine Emissions Databank (EED), either because they are legacy or do not meet the definition of thrust or technology to require regulation, the SAMPLE IV project measured the emissions from three available engines, namely a Honeywell ALF 502-R5 and 507-1H small turbofans (31 kN) and an non-regulated Pratt & Whitney PW127G turboprop engine. Planning for these tests included pre-agreeing test cycles and sampling and measurement methodologies with EASA, which were adopted in order that representative regulatory emission index (EI) nvPM number and mass data could be practicably obtained, for the purpose of comparison to regulatory nvPM limits.

To also offer 'cost effective' opportunities for other deliverables of the SAMPLE IV programme, concerned with smoke number correlations², simplified/novel measurement of nvPM³ and fuel impact nvPM correction techniques⁴, additional parallel experimentation was conducted using the same sampling and measurement methodologies reported here, with the respective data reported in the relevant deliverable reports.

2. nvPM Emissions Testing of Small Gas Turbine Engines

As part of a wider test campaign, the engine-exit emissions of two Honeywell legacy turbofan engines, the ALF502-R5 and ALF507-1H, were measured at CFS Aero at Hawarden airport in the UK. Both engines are rated to 31 kN thrust and use reverse flow annular combustors, with the ALF502 equipped with one low-pressure compressor, whereas the LF507 has two low-pressure compressors. Both engines are just above the ICAO minimum rated thrust limit of 26.7 kN and therefore have regulatory values reported for smoke and gaseous emissions in the ICAO Engine Emissions Databank, but due to their legacy nature, they have not been certified for nvPM emissions. Given their power range, it is expected that the nvPM emissions will be similar in nature to slightly lower thrust non-regulated turbofan engines.

¹ SAMPLE IV Deliverable 4 report: https://www.easa.europa.eu/sites/default/files/dfu/sampleiv_-_d4.pdf

² SAMPLE IV Deliverable 6 report: https://www.easa.europa.eu/sites/default/files/dfu/sampleiv_-_d6_0.pdf

³ SAMPLE IV Deliverable 3 report: https://www.easa.europa.eu/sites/default/files/dfu/sampleiv_-_d3.pdf

⁴ SAMPLE IV Deliverable 7 report: https://www.easa.europa.eu/sites/default/files/dfu/sampleiv_-_d7.pdf



Figure 1: photographs of test engine on the CFS aero Hawarden test stand (left), sampling probe and near-field measurement cabinet (middle), and main measurement cabin (right)

2.1. Experimental methods

2.1.1. Sampling and measurement system

As part of a wider test campaign, a dedicated exhaust probe was developed and manufactured by Scitek Consultants to allow ICAO certification-like emission sampling of the ALF502-R and ALF507-1H at the CFS Aero engine test facility. An equal area ‘piccolo’ type probe (10 mm tube with 1.5 mm wall) employing 21 (1 mm diameter) sampling points was manufactured, towards representative sampling of the exhaust. The 21 equal area sampling points were distributed from the exhaust centreline to the upper wall of the exhaust duct as shown in Figure 2 and Figure 3.

The probe was mounted within the engine exhaust jet pipe/nozzle (Figure 2), by modifying the part to include an upper and lower support boss which allowed for thermal expansion. In discussions with EASA, it was agreed that this concept nominally adhered with the requirements of A16V2 [1], which specifies the probe should sample from within $\frac{1}{2}$ a nozzle diameter, to ensure raw emissions are sampled with no entrainment of air. As can be seen in Figure 3, a tube-in-tube heat exchanger concept was designed and incorporated into the probe. The design included an exhaust ‘scoop’ in the lower half of the jet pipe/nozzle, which ensured the flow of hot exhaust gases around the internal sample line, which maintained the exhaust sample temperature as it passed through the cold bypass air. This design concept was employed to ensure compliance with the $>145^\circ\text{C}$ exhaust sample temperature defined in A16V2 [1], required to prevent condensation and PM thermophoretic loss before the sample is actively cooled in the ICAO-prescribed primary diluter stage.

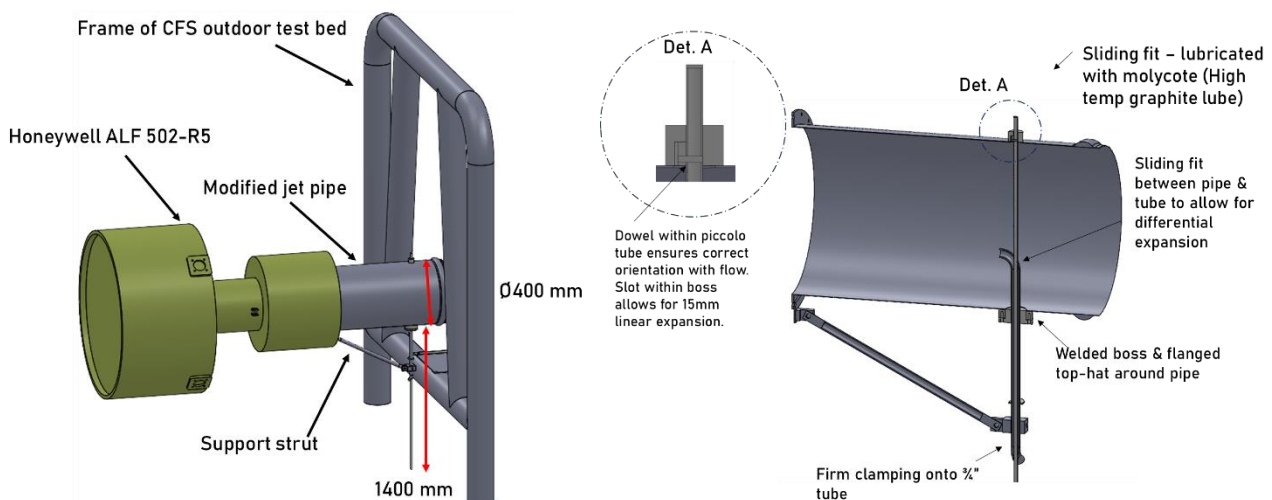


Figure 2: Diagram of the top-level assembly (left) and support arrangements (right) used on CFS Aero test bed

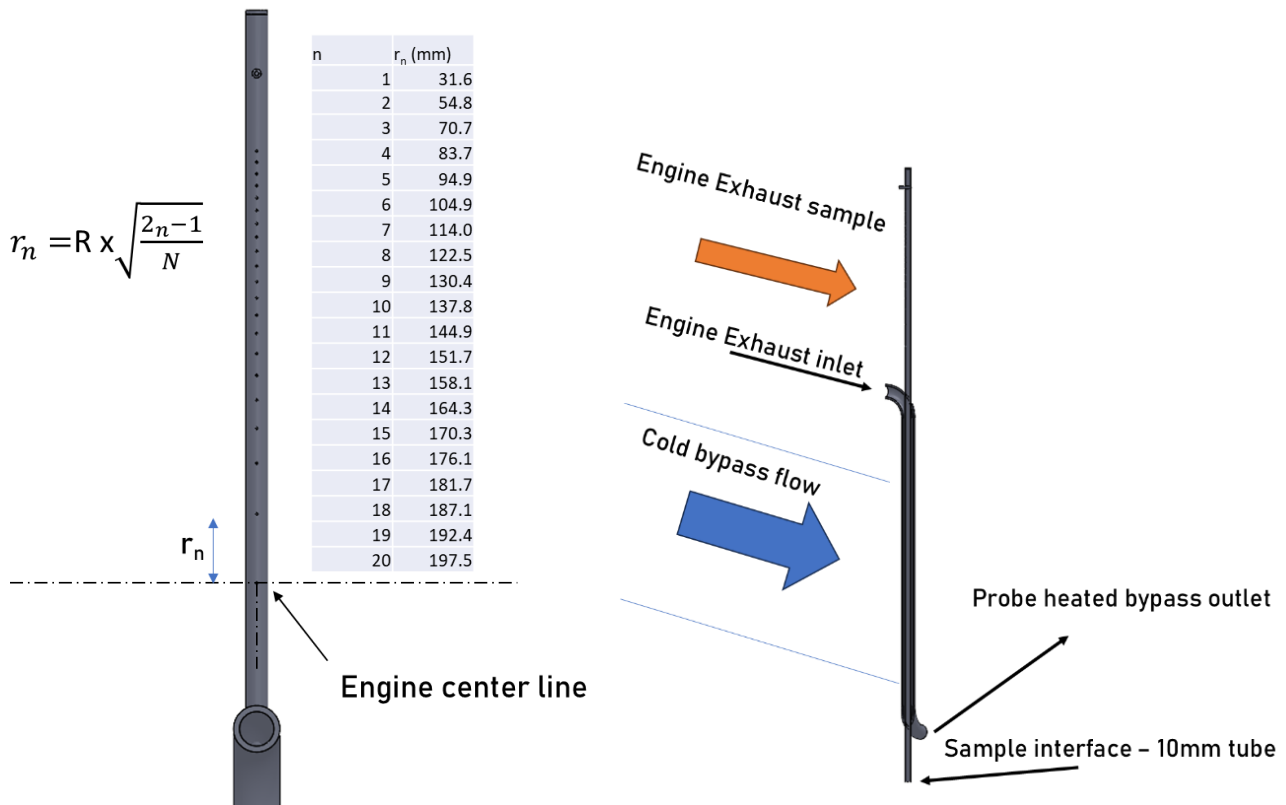


Figure 3: schematic and spatial locations of the sampling probe with the equal area sampling points (front-view left) and sample intake (side-view right)

The outlet of the probe was connected to a Y-splitter feeding the EUR nvPM sampling and measurement systems dilution box and a Dekati eDiluter™ pro used to demonstrate additional ‘novel’ measurements (see SAMPLE IV deliverable 3 report⁵), as shown in Figure 4. All sample lines up to the EUR dilution box were insulated, to maintain the inlet sample temperature. Details of the EUR nvPM reference system can be found in the literature [2], [3], [4]. Briefly, regulatory gases (CO, NO_x, THC) and smoke were measured using the raw gas line while regulatory nvPM number and mass were measured behind a Dekati DI-1000 diluter operated with nitrogen. Smoke Number (SN) was measured using a Chell CSM2001 analyser, sampling at a flowrate of 14 Lpm in accordance with ARP1179D [5]. Due to time/cost constraints only one SN sample was taken at each LTO point, although ICAO [1] specifies that the number of samples at each engine operating condition shall not be less than 3. As discussed, the measured SN was also used in understanding smoke correlation data reported in the SAMPLE IV Deliverable 6 report⁶. Additional particle size measurements were made in parallel to regulatory nvPM using a Cambustion DMS500 and Grimm SMPS+C 5420. The engine testing was conducted September 2023, with the AVL MSS (nvPM mass) and APC (nvPM number) calibrated in February 2023, while all gas instruments (THC, NO_x, CO₂) linearised in July 2023, with the calibration and linearity certificates provided in the Appendix.

DF₁ varied between 8.1 – 13.1 over the six-days of testing, while the ambient temperature and relative humidity varied between 12-22°C and 47-94%, respectively. The engine exhaust temperature (T_{EGT}), measured between the high- and low-pressure turbine rotors, varied from 127 °C, at sub-idle (<7%) thrusts, up to 600°C at maximum thrust conditions. Due to T_{EGT} not always being >160°C and the collection section between the probe and the EUR dilution box being only passively heated by the core engine flow, this meant that T₁, as newly defined in ARP6481A [6] (i.e., Splitter1 wall temperature), varied between 108 – 238°C. However, given

⁵ SAMPLE IV Deliverable 3 report: https://www.easa.europa.eu/sites/default/files/dfu/sampleiv_-_d3.pdf

⁶ SAMPLE IV Deliverable 6 report: https://www.easa.europa.eu/sites/default/files/dfu/sampleiv_-_d6_0.pdf

the EUR dilution box is heated, the aerosol entering the diluter was typically $>145^{\circ}\text{C}$, as measured by an additional thermocouple positioned between the EUR dilution box isolation valve and Diluter1 inlet (previous location of T_1 , with this temperature varying between $143 - 178^{\circ}\text{C}$, dependant on the thrust point being tested).

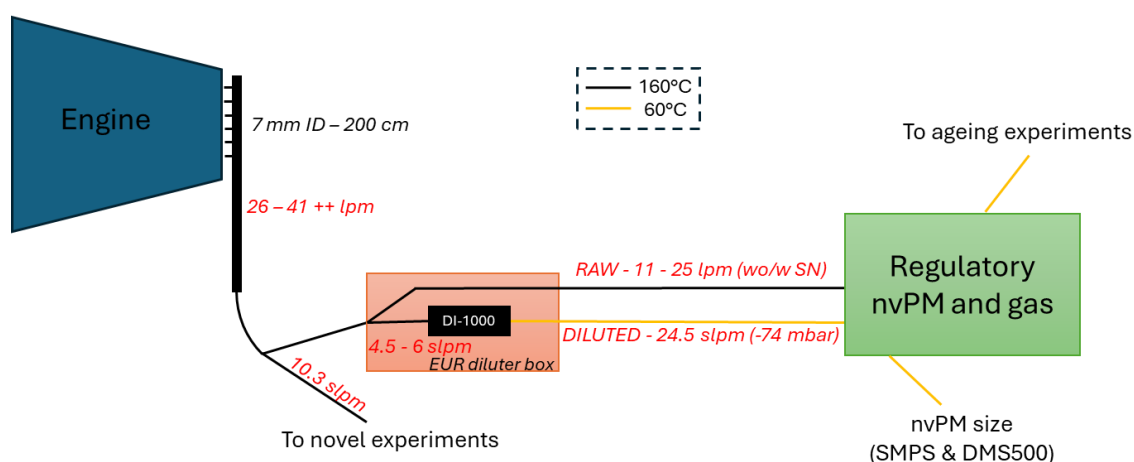


Figure 4: Simplified diagram of the full sampling and measurement system (note full details of the novel experiments setup is available in the SAMPLE IV Deliverable 3 report⁷)

Due to a rapid pressurisation of the EUR nvPM reference system sampling line during pretest shakedown measurements, as a result of an unexpected loss in power, the APC CPC was malfunctioning for the majority of the ALF502 and LF 507 tests as a result of Butanol being pushed through the CPC optics. Therefore, an additional CPC (TSI 3756 S/N: 3750185201/02) which meets the CPC specifications of ICAO A16V2 was positioned to sample in parallel, from the exhaust of the APC secondary diluter.

At the end of the test campaign, following rigorous cleaning and drying of the internal APC CPC, its output concentration was compared to the external TSI CPC, with both sampling from the secondary APC diluter, to deduce a correction function for the employed CPC. This CPC 'calibration' data is displayed in Figure 5 (a), with a derived correction factor of $1/0.8961$ applied to the additional CPC to derive a regulatory equivalent nvPM number for the whole test campaign.

The undercounting of $\sim 10\%$ from the external CPC, when compared to the internal APC CPC could be explained by the additional sample path of $\sim 1\text{m}$ causing additional diffusion loss, and the fact that the k-factor correction wasn't applied by default to the additional CPC. Figure 5 (b) displays the size-dependent differences between the two CPCs, with the overall reduction in ratio being consistent with the additional diffusional loss in the additional sampling line and the up-trend $< 15\text{ nm}$ likely caused by the higher counting efficiency of the external CPC at lower sizes (D_{90} of 10 nm Vs 15 nm respectively). Overall, the fluctuations do not exceed 1% between $15 - 40\text{ nm GMD}$, therefore a single correction factor was deemed appropriate.

It is noted that the performance of the EUR nvPM reference system CPC was further checked post-test to ensure the validity of the applied correction factor. This performance check was conducted by comparing the EUR nvPM reference system CPC against the reference CPC of a national laboratory during a VPR penetration calibration in May 2024 (see SAMPLE IV deliverable 3 report⁷). This check highlighted that no long-term damage to the EUR nvPM refence system CPC had been sustained and the correction factor derived was traceable.

⁷ SAMPLE IV Deliverable 3 report: https://www.easa.europa.eu/sites/default/files/dfu/sampleiv_-_d3.pdf

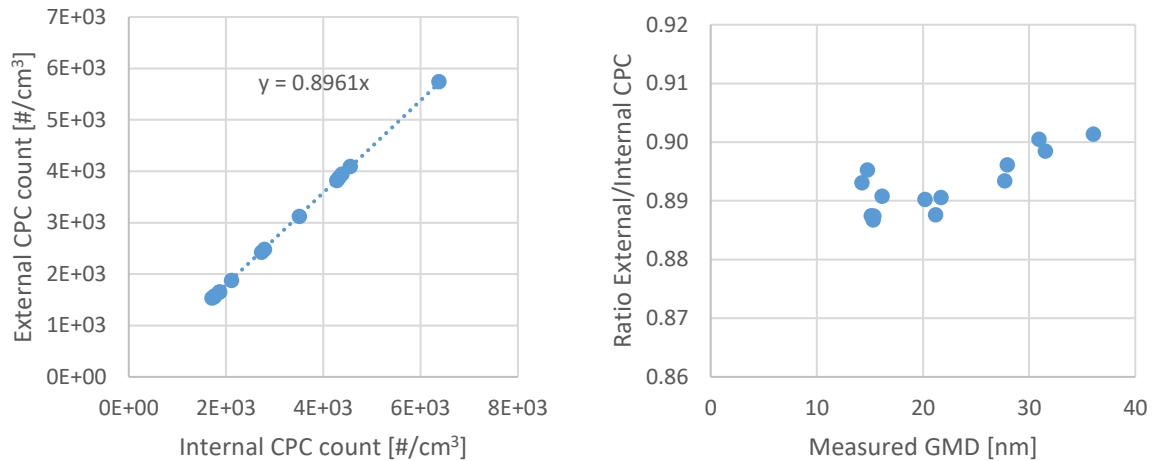


Figure 5: Number concentration comparison between additional and EUR nvPM reference CPC behind the VPR of the EUR APC during a full engine curve when sampling the ALF502

2.1.2. Determination of ICAO-equivalent LTO points & Emissions Curves

As agreed with EASA prior to the testing, LTO-equivalent test points were determined during a ‘shakedown’ test which was conducted on 15th September 2023 for the LF507 and 26th September 2023 for the ALF502 engine. During this test the engine thrust was gradually increased in steps of 5-10%, up to maximum thrust and then decreased similarly back to ground idle. Suitably corrected measurements of CO, CO₂ and NO_x, obtained using the EUR nvPM sampling and measurement system were then plotted against combustor inlet temperature (T_{30}), in order to derive LTO-equivalent engine powers by reading off equivalent T_{30} at the point the of reported EI for the given emissions species in the ICAO databank. This was considered suitable since ambient temperatures and pressures were close to ISA conditions (15 °C, 1 atm). The graphs of the NO_x, CO and THC data used to determine the LTO equivalent points are given in Figure 6, Figure 7 & Figure 8 respectively.

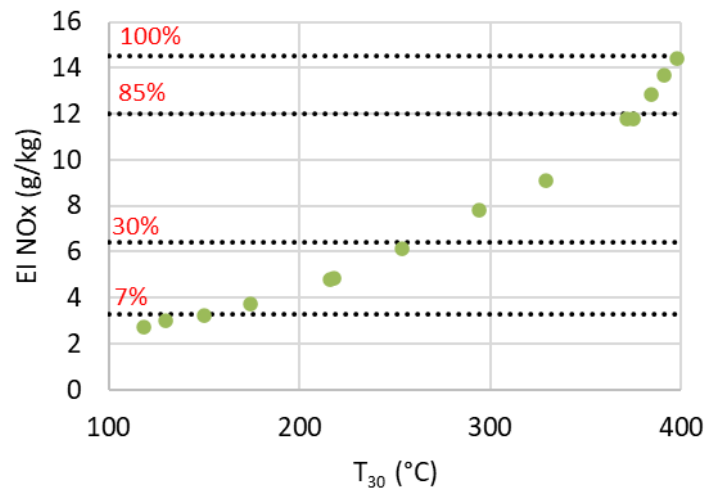


Figure 6: Measured EI NO_x during LF507 ‘shakedown’ testing highlighting equivalent T_{30} points of LTO reported values (datapoints intersecting with black dashed lines)

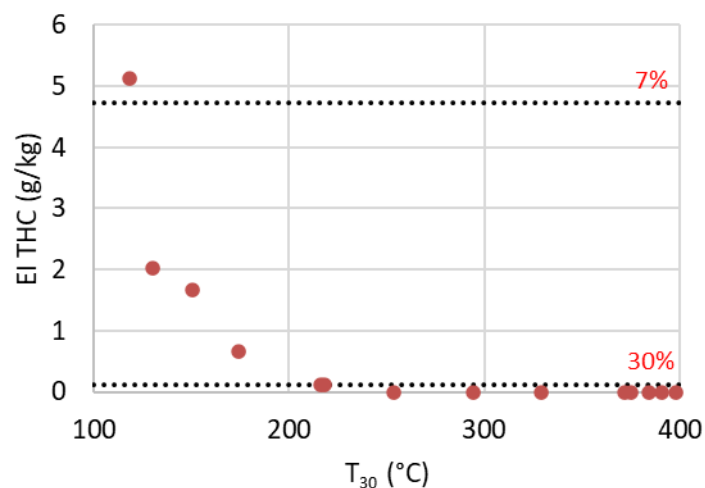


Figure 7: Measured EI THC during LF507 'shakedown' testing highlighting equivalent T_{30} points of LTO reported values (datapoints intersecting with black dashed lines) – 85% and 100% LTO points have EI THC ~ 0 g/kg

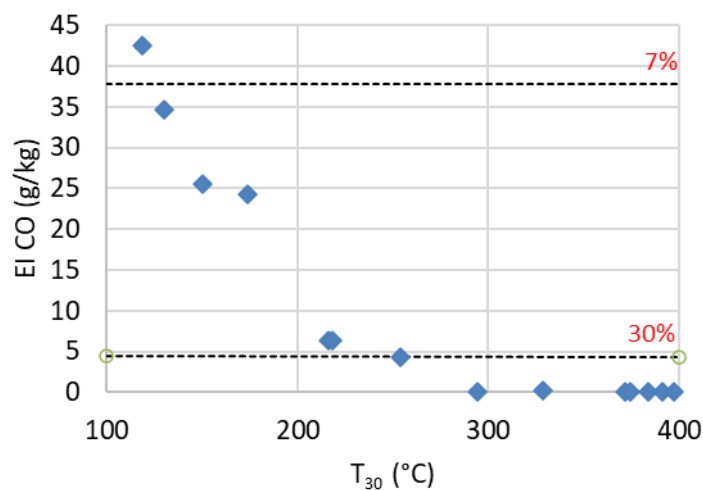


Figure 8: Measured EI CO during LF507 'shakedown' testing highlighting equivalent T_{30} points of LTO reported values (datapoints intersecting with black dashed lines) – 85% and 100% LTO points have EI CO ~ 0 g/kg

It was observed that there were slight discrepancies in the powers required to match EI NO_x and other EIs at approach (30%), as such it was decided that two approach-type conditions would be measured in subsequent test days.

As a check of nvPM emissions, DMS500 data was also recorded during the test sequence so as the overall trend of nvPM number emissions could be seen along with the witnessed particle sizes, as is shown in Figure 9. As is typical with larger engines, the particle sizes witnessed at higher powers are typically bigger, corresponding to higher mass loadings, even though the number concentration is seen to be dropping.

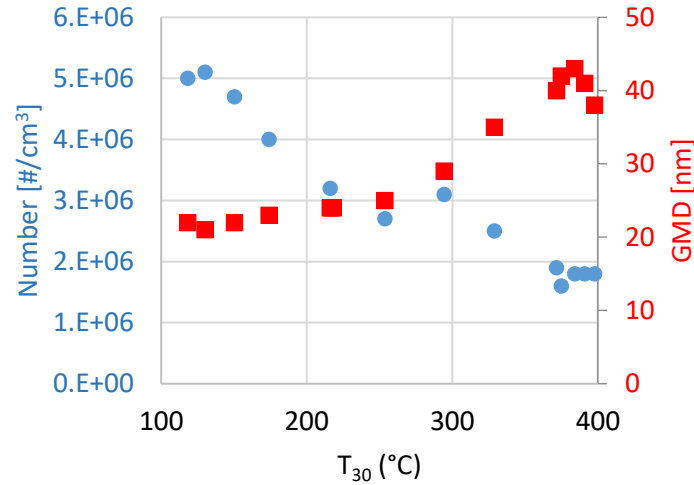


Figure 9: Measured (uncorrected) PM number concentrations (blue) and particle sizes (red) during LF507 'shakedown' testing

T_{30} equivalent temperatures for each of the LTO points (7, 30, 85 and 100%) were fixed to ensure consistency across repeated tests conducted on different days. A second order polynomial was fitted to the T_{30} versus thrust data for both engines, allowing thrust to be derived at any given T_{30} , as shown in Figure 10. It is noted that an additional 4% thrust point was assumed at the lowest measured T_{30} to better constrain and improve the polynomial fit for converting T_{30} to thrust.

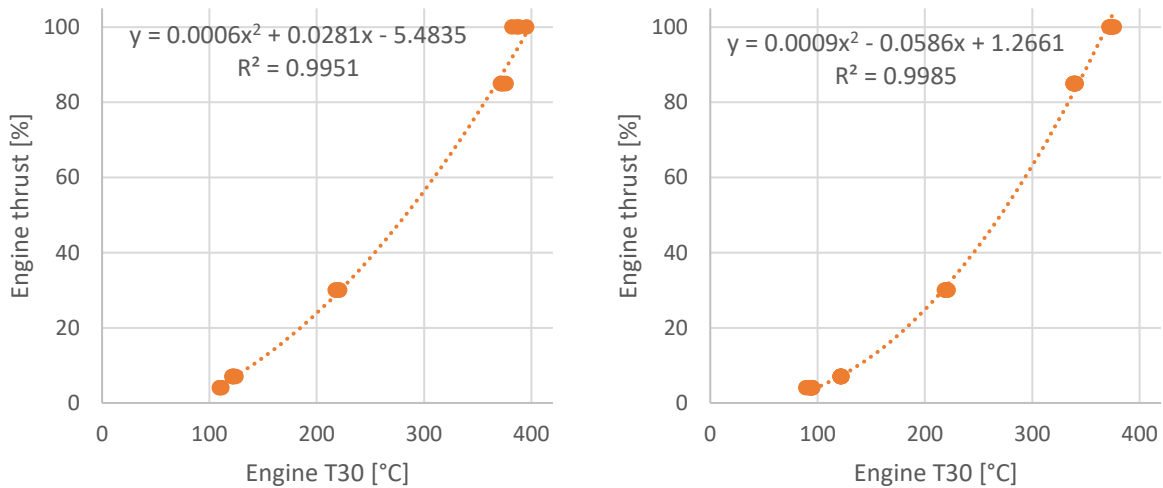


Figure 10: Engine T_{30} Vs Thrust for the LF507 (left) and ALF502 (right engines)

Following the shakedown runs, an emission curve was developed, which balanced sufficient relevant engine power conditions against available fuel. The test series was composed of up to 8 test points, driven on engine T_{30} (i.e., thrust), and repeated for each fuel and engines investigated (sometime repeated several times on the same fuels).

Emission sampling started at ground idle after a 10-minute warm-up period, with engine power then gradually increasing to take-off (up-cycle) and back to ground idle (down-cycle) as detailed in

Table 1. Each test point lasted at least 3 minutes to ensure stable emissions during the test point, with presented data derived from an average over a 30-second period from within the stable point. Smoke was taken on the LTO points on the down curve to ensure the engine was hot and stable.

Table 1: Test points achieved during LF507 and ALF502 engines emission testing with their corresponding engine power

| Test Point | Label | Approximate engine thrust [%] |
|------------|------------------------------|-------------------------------|
| 1 | Ground idle | 4-5 |
| 2 | Idle | 6 |
| 3 | Taxi (LTO) | 7 |
| 4 | Approach (LTO) | 30 |
| 5 | Approach max NO _x | 40-45 |
| 6 | Cruise | 70 |
| 7 | Climb (LTO) | 85 |
| 8 | Take-off (LTO) | 100 |

2.1.3. Fuels tested

The two Jet A fuels used for this testing were analysed by independent laboratories using ASTM approved methods, with the main properties summarised in Table 2, along with the allowable range of values specified by ICAO in Appendix 4 of A16V2 [1] for engine certification testing. Jet A (1) falls within the ICAO specifications for all measured properties. It is noted that although Jet A (2) meets the ASTM aromatics content allowance (<25%), it is just below the lower limit (13.5% Vs 15%) of permissible aromatics prescribed for engine certification testing.

Table 2: Summary of fuel properties during LF507 and ALF502 engine emission testing

| Property | Method used | Jet A (1) | Jet A (2) | ICAO Allowable range of values |
|---|------------------------|-----------|-----------|--------------------------------|
| Density at 15°C [kg/m ³] | D4052 | 795.2 | 796.6 | 780-820 |
| Distillation temperature 10% boiling point [°C] | D86 | 162.4 | 167.9 | 155-201 |
| Distillation temperature final boiling point [°C] | D86 | 238.7 | 266 | 235-285 |
| Net heat of combustion [MJ/kg] | IP12 or D3338* | 43.189* | 43.18 | 42.86-43.50 |
| Aromatics content [%v/v] | D1319 | 18.6 | 13.5 | 15-23 |
| Sulphur [ppm mass] | D4294 or D5453* | 320* | <270 | < 3000 |
| Hydrogen content [%m/m] | D3343 | 13.75 | 14.03 | 13.4-14.3 |

2.1.4. Data processing

The measured raw gaseous emissions were corrected and converted to Emission Indices (EIs) as specified in ARP1533C [7] and Attachment B in A16V2 [1] to account for water vapour, O₂ broadening, interference and conversion efficiency of the NO_x analyser. Given the THC analyser (Signal 3000HV) was calibrated on propane equivalence, it reported measured unburnt hydrocarbons in ppmC₃, therefore the measured values were multiplied by three to report in ppmC. The NO_x analyser (Signal 4000VM) was configured to measure total NO_x during this study, hence there is no speciation of NO and NO₂ in this data.

The measured nvPM number and mass concentrations were corrected and converted to EIs as specified in ARP6320A [8] and Appendix 7 in A16V2 [1] with the equations shown below. The fuel hydrogen to carbon ratio (α) was derived from the fuel hydrogen content measured by laboratories following the ASTM D3343 method, as detailed in Table 2. The thermophoretic loss correction factor k_{thermo} was calculated using T_{EGT} .

$$EI_{\text{mass}} = \frac{22.4 \times nvPM_{\text{mass_STP}} \times 10^{-3}}{\left([CO_2]_{\text{dil}} + \frac{1}{DF_1} ([CO] - [CO_2]_b + [HC]) \right) (M_C + \alpha M_H)} \times k_{\text{thermo}}$$
$$EI_{\text{num}} = \frac{22.4 \times DF_2 \times nvPM_{\text{num_STP}} \times 10^6}{\left([CO_2]_{\text{dil}} + \frac{1}{DF_1} ([CO] - [CO_2]_b + [HC]) \right) (M_C + \alpha M_H)} \times k_{\text{thermo}}$$

In this study a fuel composition correction (k_{fuel}) has not been applied. Given the very close agreement of the Jet A (1) fuel to the reference fuel hydrogen content of 13.75% compared to 13.8% (see Table 2), then correction would not meaningfully correct the reported EI's beyond the measurement uncertainties of the fuel analysis and nvPM measurements. Further details of this impact on this data are presented in the SAMPLE IV Deliverable 7 report⁸.

2.2. LF507-1H and ALF502-R5 Emissions Results

2.2.1. Gaseous and Smoke Emissions

The regulatory gaseous EI emissions from the LF507 and ALF502 when burning two Jet A fuels are reported in Figure 11. As would be expected, and in agreement with the shakedown testing, EI HC and EI CO decrease with increasing engine power as the combustion efficiency increases, while EI NO_x increases with increasing engine power indicative of a higher combustion temperature (i.e., T_{30}). As would also be expected, given the very similar net heat of combustion and fuel hydrogen contents, the different fuels display similar gaseous emissions within measurement uncertainty. These results are in line with the literature [4], [9] and agree with the emissions reported in the ICAO emission databank [10] at the LTO points for these engine types (see Table 3).

⁸ SAMPLE IV Deliverable 7 report: https://www.easa.europa.eu/sites/default/files/dfu/sampleiv_-_d7.pdf

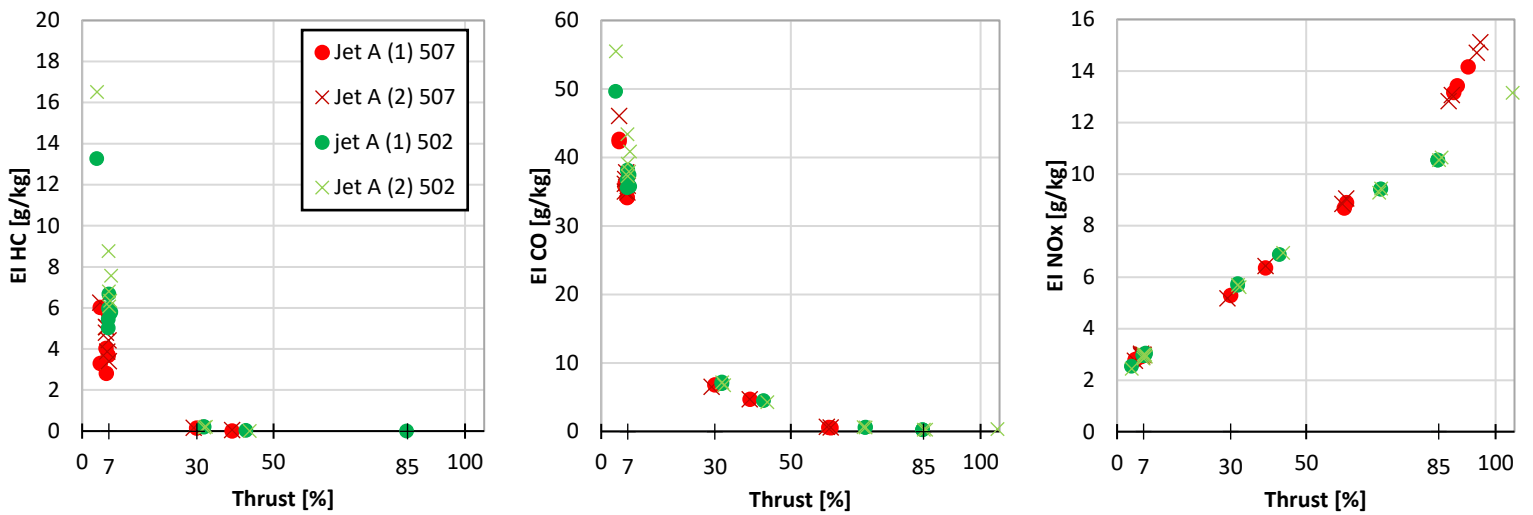


Figure 11: Regulatory HC (left) CO (middle) and NOx (right) emission indices against thrust for different fuels on the LF507 and ALF502

Table 3: Regulatory gaseous and smoke emissions for the LF507 and ALF502 copied from the ICAO emissions databank (V30)

| Engine Identification | B/P Ratio | Pressure Ratio | Rated Thrust (kN) | HC EI T/O (100%) (g/kg) | HC EI C/O (85%) (g/kg) | HC EI App (30%) (g/kg) | HC EI Idle (7%) (g/kg) |
|-----------------------|-----------|----------------|----------------------|--------------------------|-------------------------|-------------------------|-------------------------|
| LF507-1F, -1H | 5.1 | 13 | 31 | 0.01 | 0.01 | 0.12 | 4.72 |
| | | | | CO EI T/O (100%) (g/kg) | CO EI C/O (85%) (g/kg) | CO EI App (30%) (g/kg) | CO EI Idle (7%) (g/kg) |
| | | | | 0.2 | 0.3 | 4.43 | 37.83 |
| | | | | NOx EI T/O (100%) (g/kg) | NOx EI C/O (85%) (g/kg) | NOx EI App (30%) (g/kg) | NOx EI Idle (7%) (g/kg) |
| | | | | 14.52 | 12.02 | 6.39 | 3.28 |
| | | | SN Max SN T/O (100%) | SN T/O (100%) | SN C/O (85%) | SN App (30%) | SN Idle (7%) |
| | | | 10.6 | 10.3 | 10.2 | 6.9 | 6.8 |
| | | | | HC EI T/O (100%) (g/kg) | HC EI C/O (85%) (g/kg) | HC EI App (30%) (g/kg) | HC EI Idle (7%) (g/kg) |
| ALF 502R-5 | 5.6 | 12 | 31 | 0.06 | 0.05 | 0.22 | 5.39 |
| | | | | CO EI T/O (100%) (g/kg) | CO EI C/O (85%) (g/kg) | CO EI App (30%) (g/kg) | CO EI Idle (7%) (g/kg) |
| | | | | 0.3 | 0.25 | 7.1 | 40.93 |
| | | | | NOx EI T/O (100%) (g/kg) | NOx EI C/O (85%) (g/kg) | NOx EI App (30%) (g/kg) | NOx EI Idle (7%) (g/kg) |
| | | | | 13.35 | 10.56 | 6.6 | 3.78 |
| | | | SN Max SN T/O (100%) | SN T/O (100%) | SN C/O (85%) | SN App (30%) | SN Idle (7%) |
| | | | 15.4 | 13.5 | 12.7 | 5.7 | 2.3 |

The raw CO₂ emissions measured and corrected as per A16V2 [1], are presented in Figure 12. As would be expected at the higher fuel flows witnessed at higher thrusts, an increase in CO₂ is witnessed corresponding with a reduced Air-to-fuel ratio.

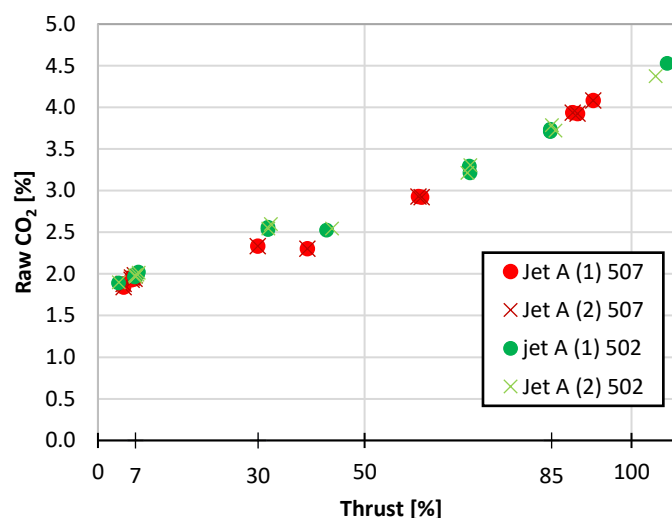


Figure 12: Corrected raw CO₂ emissions against thrust for different fuels on the LF507 and ALF502

Smoke Number (SN) measurements are displayed in Figure 13 for the two fuels investigated, again noting that only one measurement was taken at each LTO test point during the down-curves. SN is seen to typically increase with power for both engines, in line with the nvPM mass trends reported later in section 2.2.2. Although, for the LF507, SN was found to be higher at 7% than at 30% for the Jet A (1) case, which is likely associated with the measurement uncertainty. These SN trends are in line with the nvPM mass trends reported in section 2.2.2.

As can be seen in Figure 13, the measured SN are compared to the reported SN values from ICAO emissions databank (see Table 3). It is noted that the first test fuel, Jet A (1), had a similar H/C ratio to the data reported in the emissions databank (1.93), as such it would be expected that similar SN's would be measured. To aid comparison, error bars of ± 3 are added to the measured SN values in Figure 13, representing the achievable precision of SN [5]. It is seen that the measured and ICAO emissions databank SN follow the same trends for both engines, with the data reported in the databank typically higher than the SN's measured during this campaign, but generally within the reported uncertainty of measurement.

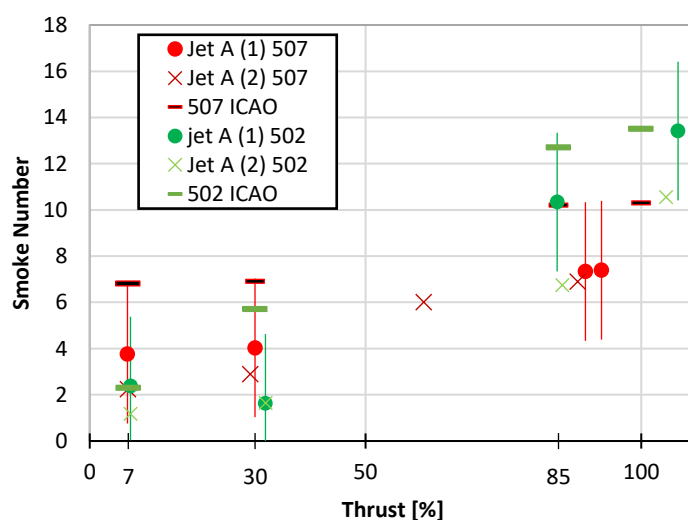


Figure 13: Measured Smoke number against thrust for the LF507 and ALF502 engines

2.2.2. nvPM Emissions

El nvPM number and mass as specified by ICAO A16V2 [1] are presented in Figure 14. For both engines, the maximum nvPM El number emissions occur at the lowest thrust, decreasing to reach a minimum at the highest thrusts measured. As can be seen, particularly in the case of the LF507, the nvPM El mass displays a U-shape, with emissions first decreasing from low to mid thrust and then increasing again. For the 507, the maximum nvPM El mass occurs at the lowest sub idle powers, indicative of the inefficiencies witnessed at these points as supported by the elevated El HC and El CO emissions also witnessed (Figure 11). However, in the case of the ALF502 the maximum nvPM El mass was witnessed at the highest measured power.

The typically lower nvPM El emissions with Jet A (2) when compared to Jet A (1) can be attributed to its higher hydrogen content (14.03 Vs 13.75% - see Table 2), in line with the literature [3], [4], [11].

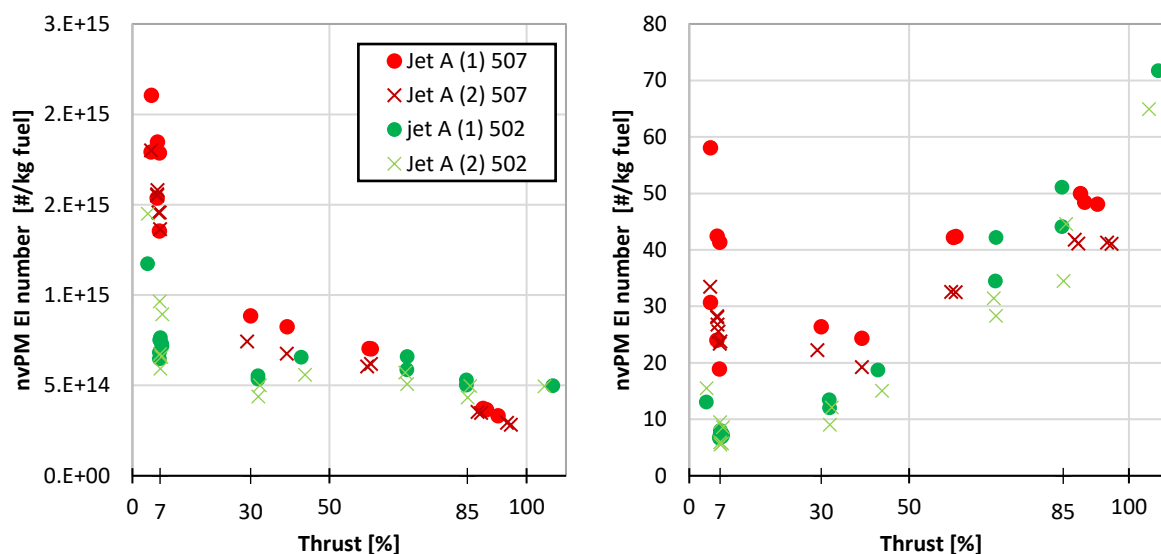


Figure 14: nvPM El number (left) and El mass (right) against thrust for the LF507 and ALF502

Additionally, the certification-equivalent nvPM El number and mass data for the LF507 and ALF502 taken with Jet A (1) during the down curve is provided below in Table 4. Jet A (1) was selected given its hydrogen content is closest to the ICAO reference of 13.8% and it meets the aromatic content requirements of certification fuel [1].

Table 4: Regulatory-equivalent nvPM El emissions for the ALF 507 and 502

| Engine Identification | nvPM Elmass T/O (mg/kg) | nvPM Elmass C/O (mg/kg) | nvPM Elmass App (mg/kg) | nvPM Elmass Idle (mg/kg) | nvPM Elmass Max (mg/kg) |
|-----------------------|-------------------------|-------------------------|-------------------------|--------------------------|-------------------------|
| LF507-1H | 48.1 | 48.5 | 26.4 | 18.9 | 58.1 |
| ALF 502R-5 | 71.7 | 51.1 | 12.1 | 7.2 | 71.7 |
| | nvPM Elnum T/O (#/kg) | nvPM Elnum C/O (#/kg) | nvPM Elnum App (#/kg) | nvPM Elnum Idle (#/kg) | nvPM Elnum Max (#/kg) |
| LF507-1H | 3.33E+14 | 3.65E+14 | 8.85E+14 | 1.35E+15 | 2.11E+15 |
| ALF 502R-5 | 4.98E+14 | 5.32E+14 | 5.36E+14 | 7.52E+14 | 1.17E+15 |

Regulatory nvPM El emissions are corrected for thermophoretic losses in the collection section; However, they do not currently account for size-dependent losses within the sampling and measurement system (see SAMPLE IV Deliverable 3 report⁹). Utilising the measured-PSD-based system loss correction methodology (PSD_B)

⁹ SAMPLE IV Deliverable 3 report: https://www.easa.europa.eu/sites/default/files/dfu/sampleiv_-_d3.pdf

discussed in SAMPLE IV Deliverable report 3⁸ and Durand et al. [12], and applying it to the EI's reported above, the engine exit nvPM EI number and mass emissions for the LF507 and ALF502 are given in Figure 15.

The fully loss-corrected EI data exhibit similar shapes as the regulatory EI data, with higher concentrations, particularly at low thrust. The decrease in nvPM number and increase in nvPM mass with increasing power is explained by the increase in nvPM size, as shown in Figure 16, meaning there are fewer larger particles as the engine power increases.

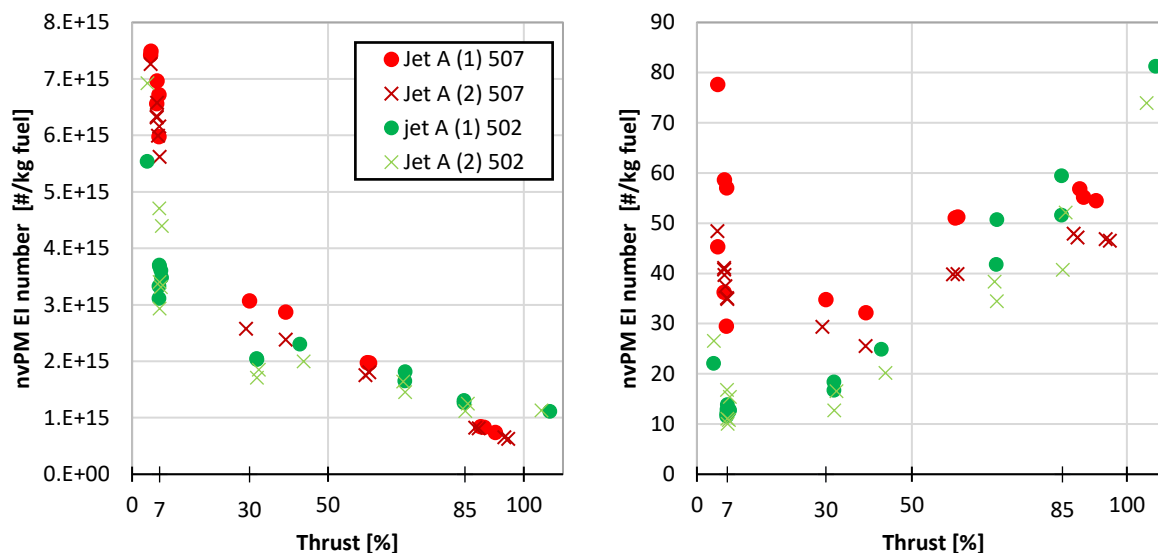


Figure 15: Loss-corrected nvPM EI number (left) and EI mass (right) emissions against thrust for the LF507 and ALF502 engines

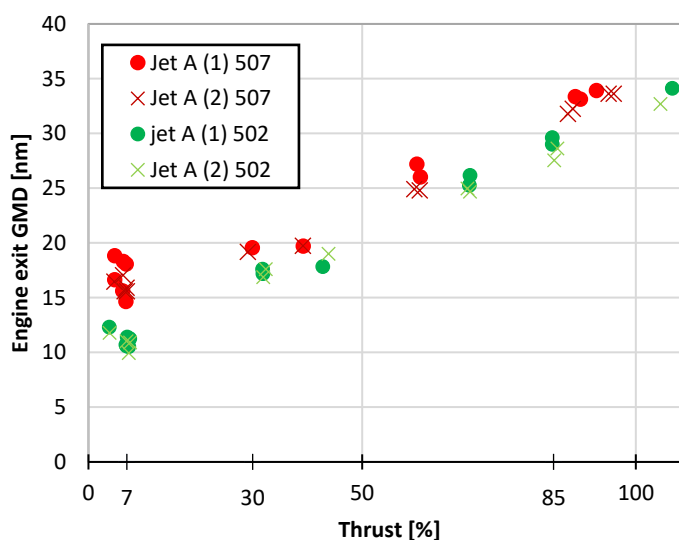


Figure 16: Engine exit Geometric Mean Diameter (GMD) derived from a Grimm SMPS+C 5420 against thrust for the LF507 and ALF502 engines

3. Emissions Testing of Non-regulated Turboprop engine

A PW127G fitted on an Airbus C-295 aircraft was tested at INTA facilities, Madrid Spain in October 2024. The PW127G is a turboprop engine developed by Pratt & Whitney Canada, and part of the PW100 series. It is designed to deliver a maximum mechanical power output of 2,130 shaft horsepower and, given it is a turboprop, is currently non-regulated in terms of emissions.

3.1. Experimental methods

3.1.1. Sampling and measurement system

3.1.1.1. Probe design

In consultation with EASA, a dedicated probe was designed to measure the emissions of the PW127G at INTA. It consisted of two single-point probes (internal diameter 8 mm, thickness 1 mm) mounted within a larger pipe (internal diameter 40 mm, thickness 2 mm), as shown in Figure 17.

The outer pipe was designed to act as a heat exchanger, ensuring the flow of hot exhaust gases over the inner sampling probes, to maintain their internal gas temperatures. All components were made of stainless steel 316L. The probe was fitted with a thermocouple at the bottom of the probe tip to record a probe-inlet exhaust temperature, firstly necessary to determine whether the probe was in the engine exhaust gas stream, and to afford PM thermophoretic loss estimations. A second thermocouple was fitted near the probe outlet at a location between the inner tubes. This temperature was recorded to monitor the exhaust aerosol temperature before reaching the dilution system.

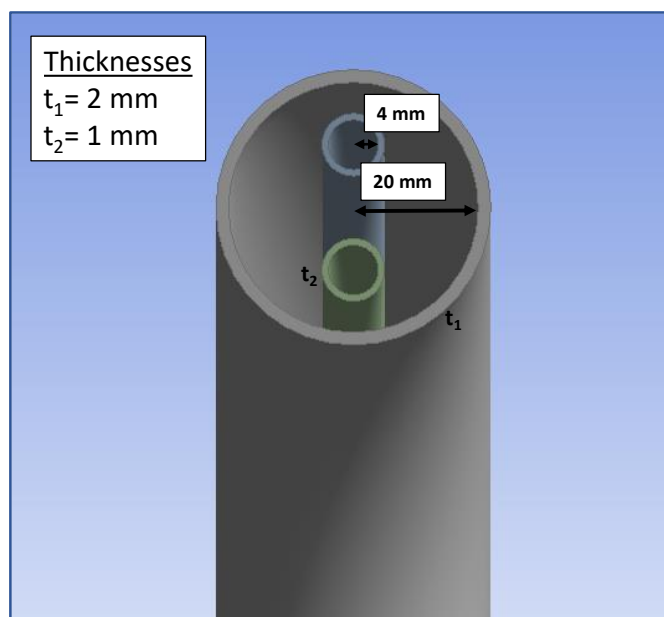


Figure 17: Diagram of the dedicated INTA probe used during PW127G emissions testing

The probe was bent at a 71° angle to allow for representative sampling from the exhaust nozzle of the PW127G engines which are oriented at 19° down from the horizontal, as can be seen in Figure 18.

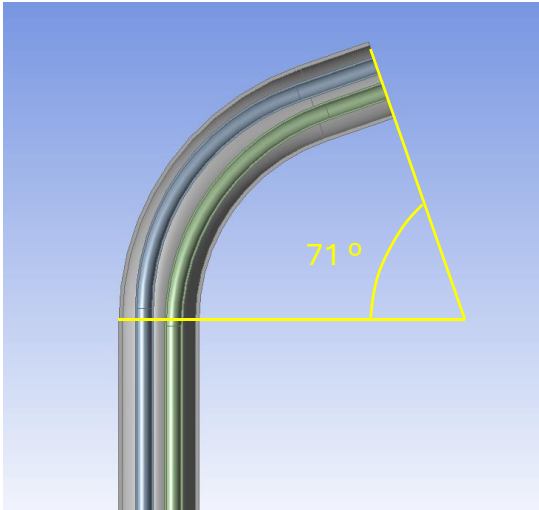


Figure 18: Diagram (left) and picture (right) of the dedicated INTAO probe orientation towards the engine exhaust

The probe was 2170 mm long and mounted on a ‘heavy-weight’ structure that allowed it to be adjusted up and down depending on the sampling position required, as depicted in Figure 19. Once set, the probe remained in the same position for the duration of the tests. A cabinet, which was manufactured as part of the base of the probe-mount structure, was also used to house some of the measurement instruments close to the engine exit.

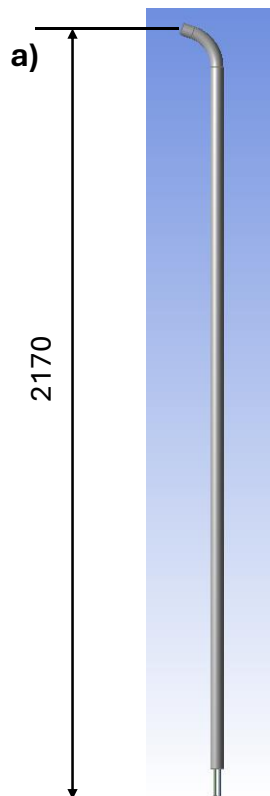


Figure 19 Diagram of the dedicated INTA probe length (left) and picture of probe mounted on the structure (right)

The probe was fixed to the structure via a reinforced stainless-steel beam to minimise vibrations and to provide rigidity to the probe. To resist any axial movement when subjected to the thrust from the engine, the structure was supported with 4000 kg of concrete ballast. Figure 20 shows pictures of the structure prior to the test.



Figure 20: Pictures of the INTA dedicated probe and structure with concrete ballast used to weight down the structure

It is noted that although the probe was designed to sit within the exit of the engine exhaust nozzle, during the engine emissions testing the probe was actually located 15 cm away from the engine-exit plane, at the request of the aircraft owner to ensure there was limited risk of damage to the aircraft's engine/exhaust should the aircraft suddenly move and make contact the stationary test probe.

3.1.1.2. Sampling system

Due to technical and planning issues associated with transporting and using the EUR or Swiss reference nvPM system for the PW127G testing, a non-compliant 'novel' sampling and measurement system as demonstrated on the aforementioned LF507 and ALF502 test was developed, with further details of these 'novel' measurements detailed in the SAMPLE IV deliverable 3 report¹⁰.

A schematic of the sampling and measurement system used during the PW127G test is given in Figure 21. As can be seen, one of the probe outlets was directly connected to the CO₂/CO analyser (Emerson) using a 25 m heated line maintained at 60 °C to suppress condensation, with a back purge installed to prevent probe contamination during engine startup and shutdown. The second probe outlet was connected to a Dekati eDiluter™ pro via a heated line set at 160°C in accordance with ICAO Annex 16 Volume II appendix 7. Following calculations of expected emissions, the eDiluter™ pro was set to dilute at 15:1 in the 1st stage (heated at 60°C) and 150:1 in the second stage (cold) with nitrogen gas used to minimise the nucleation of water/volatiles, whilst also trying to maintain the CPCs in single count mode.

Some of the emissions measurements were performed behind the first heated stage of the eDiluter™ pro (15:1 dilution), namely PSD using a TSI SMPS, located inside the aforementioned cabinet at the base of the probe stand, and an Artium LII-300 to measure nvPM mass, and a LI-COR 850 (pressure compensation control between 50 – 110 kPa) to measure diluted CO₂, which were connected to the dilution stage using a 25m heated line set at 60°C. Additionally aerodynamic size was also measured using a Dekati ELPI+ in parallel with the LII-300 and LI-COR 850.

The TSI SMPS was composed of a nano-DMA (model 3085), a CPC (model 3775 with a D₅₀~4 nm and D₉₀~10 nm), a classifier (model 3082) and a radioactive neutraliser (model 3088). Due to the limited space available in the probe stand cabinet, the SMPS CPC was located on top of the nano-DMA, with a tube length of 75 cm connecting them. Additionally, number concentrations were measured using CPCs (i.e., Grimm CPC 5421 (with catalytic stripper) and 5420, respectively) sampling behind the second stage of the eDiluter pro (150:1 dilution) to remain in single-counting mode.

To meet the definition of nvPM, as per ICAO A16V2 [1], the nvPM CPC was fitted with a Catalytic Instruments catalytic stripper heated at 350°C to ensure volatile removal. Pictures of instruments and heated sampling lines can be found in Figure 22.

¹⁰ SAMPLE IV Deliverable 3 report: https://www.easa.europa.eu/sites/default/files/dfu/sampleiv_-_d3.pdf

It is noted that both CO₂ instruments were spanned with Zero and span gas at the start of the testing, using a 4% and 4000 ppm CO₂ span gas for the raw and diluted CO₂ analysers respectively.

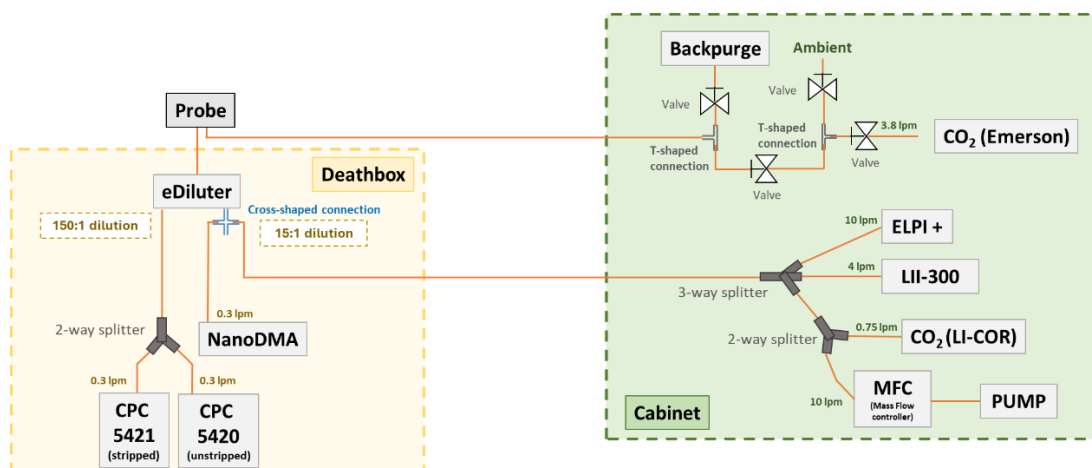


Figure 21: Diagram of the experimental set up used to measure the emissions of the PW127G

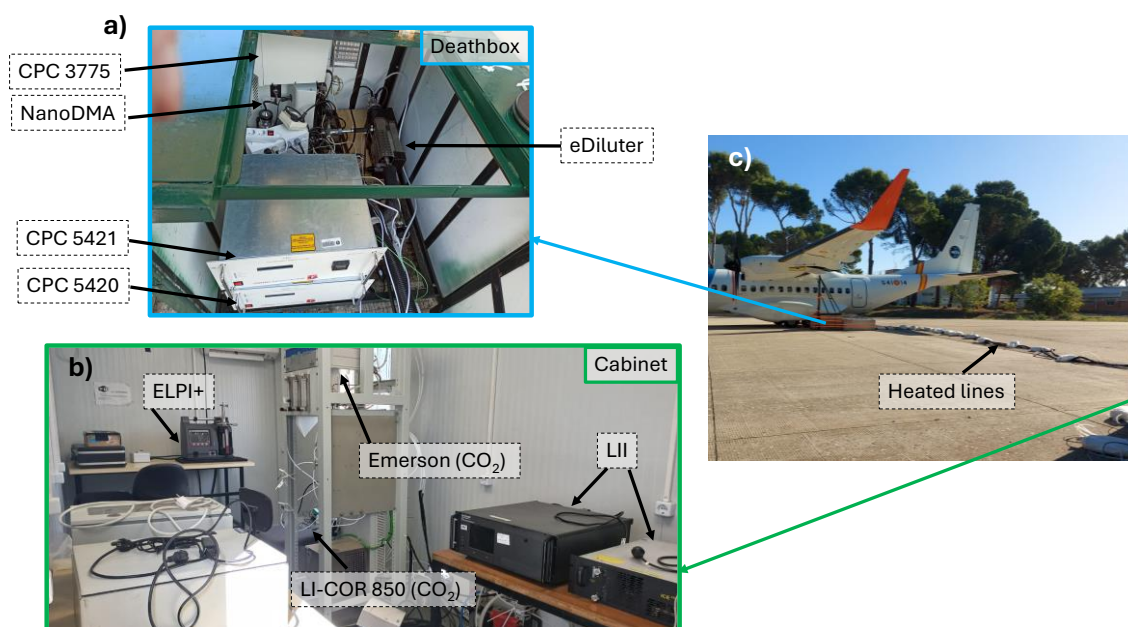


Figure 22: Pictures of a) Instruments located in the death box, b) Instruments located in the cabin, c) Heated lines

Details of the sample line dimensions and materials used to connect the different instruments are listed in Table 5. The flowrates and main characteristics for the instruments used during these tests are given in Table 6.

Table 5: Dimensions and materials of the sample lines installed

| Devices connected | Material | Internal Diameter(mm) | Length (cm) |
|---------------------|-------------------|-----------------------|-------------|
| Probe – Emerson | Stainless steel | 8 | 2500 |
| | Teflon tubing | 6 | 202 |
| Probe – eDiluter | Stainless steel | 8 | 200 |
| eDiluter – CPC 5420 | Conductive tubing | 11(0.44’') | 4 |
| | Conductive tubing | 8 (0.31’') | 4 |
| | Conductive tubing | 5 (0.19’') | 78 |
| eDiluter – CPC 5421 | Conductive tubing | 11(0.44’') | 4 |
| | Conductive tubing | 8 (0.31’') | 4 |
| | Conductive tubing | 5 (0.19’') | 78 |
| eDiluter - NanoDMA | Stainless steel | 10 | 14 |
| | Stainless steel | 6.35 (1/4’') | 14 |
| | Conductive tubing | 5 (0.19’') | 65.2 |
| eDiluter – S1 | Stainless steel | 10 | 14 |
| | Stainless steel | 6.35 (1/4’') | 14 |
| | Stainless steel | 10 | 2500 |
| S1 – ELPI+ | Conductive tubing | 11(0.44’') | 510 |
| | Conductive tubing | 8 (0.31’') | 7.9 |
| | Conductive tubing | 5 (0.19’') | 4.8 |
| S1 – LII | Conductive tubing | 11(0.44’') | 3 |
| | Conductive tubing | 8 (0.31’') | 52 |
| | Conductive tubing | 5 (0.19’') | 10.9 |
| S1 – S2 | Conductive tubing | 8 (0.31’') | 4.9 |
| | Conductive tubing | 5 (0.19’') | 70.2 |
| S2 – LI-COR | Conductive tubing | 4.7(0.44’') | 4.7 |
| | Conductive tubing | 68 (0.31’') | 68 |
| | Conductive tubing | 15 (0.19’') | 15 |
| S2 – MFC | Conductive tubing | 4.7(0.44’') | 2.9 |
| | Conductive tubing | 68 (0.31’') | 96 |

Table 6: Flowrates and properties of the instruments used in the experimental campaign (flowrate was measured using a TSI 4140 flowmeter)

| Instrument | Parameter | Theoretical Flowrate (L/min) | Max. Concentration (single count mode) | Detection limits | Measured Flowrate (L/min) |
|-------------------------------|-----------------|------------------------------|--|---------------------|---------------------------|
| CPC 5420 | nvPM number | 0.3 | 1.5E5 #/cm ³ | 4 nm | 0.29 |
| CPC 5421 | tPM number | 0.3 | 1.5E5 #/cm ³ | 4 nm | 0.29 |
| SMPS | PM size | 0.3 | >1E6 #/cm ³ | 4-250 nm | 0.26 |
| Emerson (CO ₂) | CO ₂ | 4 | 4 % | 1.5 ppm | 3.85 |
| LI-COR 850 (CO ₂) | CO ₂ | 0.75 | 2% | 1.5 ppm | 0.68 |
| ELPI+ | PM size | 10 | 8E7 #/cm ³ | 6 nm – 10 µm | 9.67 |
| LII | nvPM mass | 4 | 100 mg/m ³ | 1 µg/m ³ | 4.35 |

The ambient temperature during the test, which happened on the 18th of October 2024, fluctuated between 10-15 °C. The probe inlet thermocouple recorded engine-exhaust temperatures from 20°C of up to 391°C, as shown in Figure 23. This suggests that the 15 cm offset of the probe resulted in sampling propellor-diluted exhaust at ≤50% shaft power, except on the up-cycle of curve 1 (see details on the test matrix in section 3.1.2). This discrepancy between curve 1 and later curves is indicative that either the aircraft, probe or thermocouple slightly moved during curve 1. It is again noted that the thermocouple was located at the bottom of the probe, meaning it could be subject to the propeller wash while the raw gas and PM probe inlets, which are a few centimetres higher, may still be sampling core exhaust.

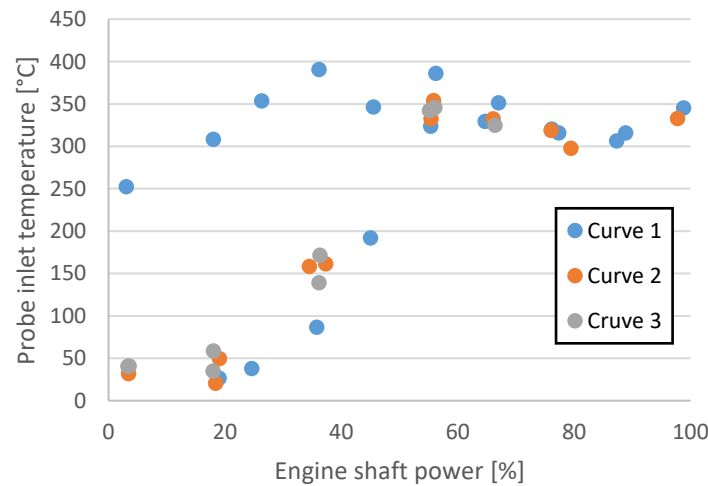


Figure 23: Probe inlet temperature representing engine-exhaust temperature plotted against engine shaft power for three up and down curves

3.1.2. Test Matrix

Following discussion with the relevant technical experts at EASA an engine test matrix was agreed, whereby the aircraft engine was cycled through an up-and-down cycle, starting at a low shaft power ramping up to 100% in power increments of 10-15%. The actual test curves tested are shown in Figure 24, highlighting that the lowest power achievable on the day was 3% and that three up-down curves were performed. It is seen that curve 1 was the longest, with tests conducted at 10 engine power levels, whereas curve 2 only incorporated 7 powers, and the final curve 3 could only achieve 5 powers due to time and fuel constraints.

The normalised shaft power presented here is defined as the product of the normalised torque and the normalised high-pressure spool speed (N_H), with all values then presented as a percent of maximum shaft power.

While the actual shaft power is proportional to the product of torque and rotational speed, since both values are already normalised, their product directly gives a normalized (percentage) shaft power.

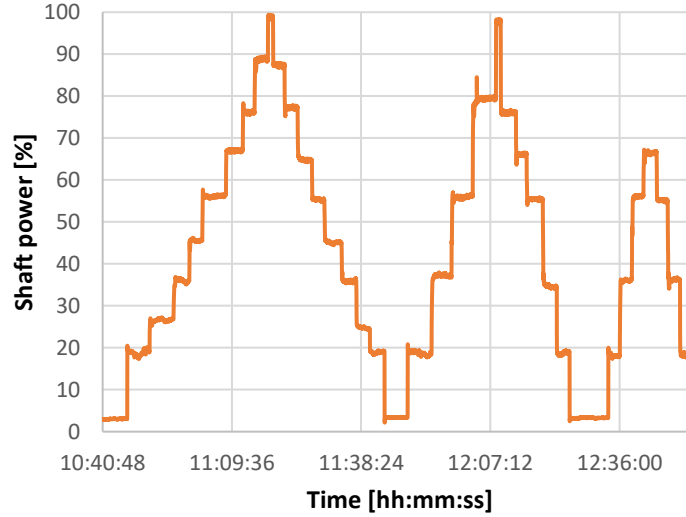


Figure 24: Timeseries of the PW127G shaft power on 18th October 2024

3.1.3. Data processing

As the first stage of the data analysis, all the instruments measuring emissions and the engine log data were first aligned temporally (to adjust for offsets in sampling time, internal clocks etc.), by peak matching. Once the datasets were satisfactorily aligned, 1-minute stable test points were selected within the 3-4 minutes steady state engine condition. The SMPS PSD scan was set for 50 seconds (with a 10 second retrace time) at an aerosol flow of 0.3 Lpm and a sheath to aerosol flow ratio of 5:1. Given the PW127G is a turboprop engine, instead of nominal thrust (%) as is used for regulated engines, the correlating engine parameter used in these results is that of engine shaft power. As discussed, it was calculated as the product of the engine torque and the high-pressure spool speed (N_H).

Given the novel sampling and measurement system used, the PM EI, which were derived from the simplified regulatory nvPM EIs [8], were calculated as followed:

$$PM EI_{num}[\#/kg_{fuel}] = \frac{22.4 \times PM_{num_STP} \times 10^{12}}{\left([CO_2]_{dil1} - \frac{[CO_2]_b}{DF_1}\right)(M_c + \alpha M_H)} \times k_{thermo}$$

$$PM EI_{mass}[mg/kg_{fuel}] = \frac{22.4 \times PM_{mass_STP}}{\left([CO_2]_{dil1} - \frac{[CO_2]_b}{DF_1}\right)(M_c + \alpha M_H)} \times k_{thermo}$$

Where PM_{num_STP} is the number concentration reported from either CPC5420 (tPM), CPC5421 (with built-in, internal, catalytic stripper - nvPM) or SMPS (tPM) at STP, PM_{mass_STP} is the mass concentration from either measured LII-300 (nvPM) or derived from the SMPS (volume x assumed effective density – tPM) at STP, $[CO_2]_{dil1}$ is gas concentration of CO_2 at the 1st eDiluterTM pro stage in ppm, $[CO_2]_b$ is the background CO_2 level in ppm (measured at ~450 ppm by the LI-COR 850), DF_1 is the 1st eDiluterTM pro stage dilution factor, M_c is the molar mass of carbon (12.01 g/mol), M_H is the molar mass of hydrogen (1.008 g/mol), α is the fuel H/C content, and k_{thermo} the thermophoretic loss correction factor in the collection section.

Given the fuel H/C wasn't directly measured for the fuel in the aircrafts fuel tanks, a value of 1.93 for α was used as it represents the average for Jet A aviation fuels (i.e., FHC of 13.8%). k_{thermo} ranged between 1 and 1.18 for this test campaign and was calculated using the probe inlet and outlet temperatures. Standard temperature corrections were applied to the CPC 5420, CPC 5421 and SMPS number and mass concentration given they are calibrated and report at 21.1°C (correction of $294.25/273.15=1.08$).

When using the CPC 5240 and 5421 number concentration to calculate EIs, an additional dilution-correction factor of 10 is applied to correct for the difference in dilution between the 2nd and 1st Ediluter stage, from which the diluted CO₂ measurement was made. Also, when using the CPC 5240 (nvPM) specifically, additional losses in the catalytic stripper were also corrected for, using previous empirically derived size dependant loss factors.

The PM mass from the SMPS was derived by converting the measured number-space particle size distribution into volume space with sphericity assumed, fitting a lognormal distribution to it, and integrating to calculate a total volume undersize. The mass was then derived by multiplying the total volume by a particle effective density, which was deduced using the density correlation, formulated empirically across many gas turbine engines, proposed by Durdina et al. [13].

It is noted that the PM EIs as calculated above are expected to be comparable to fully loss-corrected (i.e., with k_{SL}) EIs given the much shorter sample line length, and therefore negligible size-dependent losses in this novel sampling and measurement system. Hence, to provide a prediction of ICAO defined nvPM EI, k_{SL} number and mass for the additional sampling lines and VPRs must be deducted to result in the relatively lower EI's that would be expected at the end of a compliant sampling system.

3.2. Emissions Results

3.2.1. Gaseous emissions

The raw and diluted CO₂ are shown in Figure 25 against engine shaft power. As can be seen the CO₂ steadily increased with engine power up to ~55% shaft power and then stabilises, even though the fuel consumption steadily increases up to 100%, as can be seen in Figure 26. This trend is different to that typically noted for turbofans (Figure 12). This suggests that from >55% shaft power, the AFR of the combustor remains relatively constant.

Significant scatter is observed for the diluted CO₂ < 30% shaft power, indicating that the emissions probe, located 15 cm from the exhaust nozzle, was maybe sampling at the boundary of the core exhaust, while the spatially higher "raw CO₂" probe was likely still sampling at the core exhaust.

This is further highlighted in Figure 26 (b) reporting the measured 1st stage eDiluter™ dilution ratio (i.e., DF₁); For shaft powers >40%, the measured DF₁ is around 14:1, in-line with the eDiluter™ setting, and in compliance with A16V2. For shafts powers <40%, the measured DF₁ fluctuates between 15 and 35, suggesting both probes are not sampling the same exhaust, if it is assumed that the eDiluter™ pro is remaining constant, as it was shown to do in the earlier LF507/ ALF502 testing.

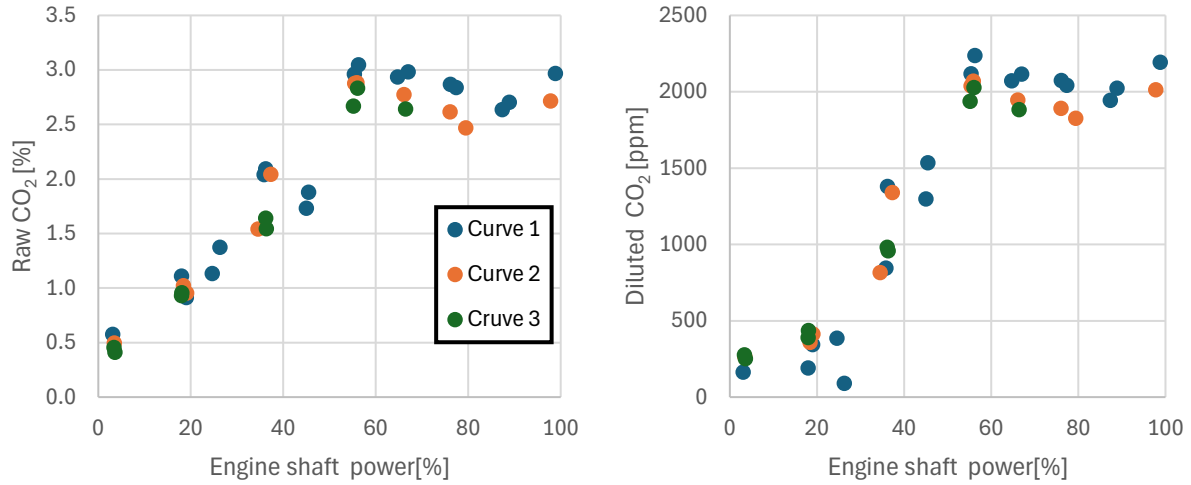


Figure 25: CO₂ measured on the raw probe (left) and diluted probe behind the 1st stage of the eDiluter pro (right) against engine shaft power

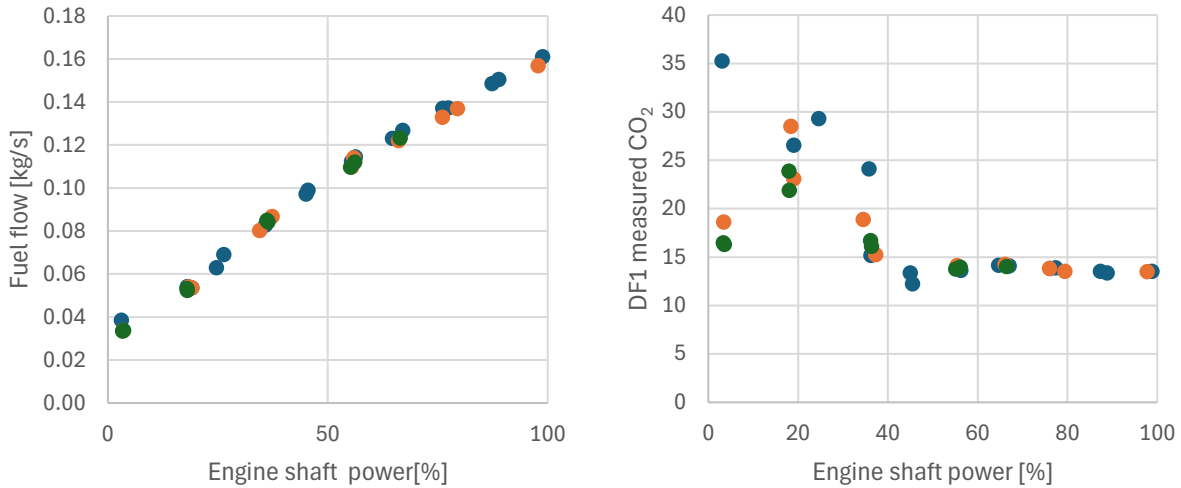


Figure 26: Fuel flowrate (left) and measured DF₁ (right) against engine shaft power

3.2.2. PM emissions

The PM (tPM) emissions as measured by the SMPS sampling behind the 1st dilution stage (in parallel to the diluted CO₂ measurement) and the 5420 CPC behind the 2nd dilution stage, were first compared, as shown in Figure 27. As can be seen, the instruments trend linearly, with a measured ratio of approximately 7:1, while a ratio of 10:1 was expected in theory (i.e., difference between 1st and 2nd stage dilution 15:1 and 150:1). This ratio suggests that either the SMPS is counting less than expected by approximately 40%, or that the 2nd dilution stage is not diluting as much as expected. Some of the scatter around the trendline can be attributed to the fact that the SMPS PSD requires a 1-minute scan, while the CPC records at 1 Hz, with the processed test points not precisely matching the SMPS scan times.

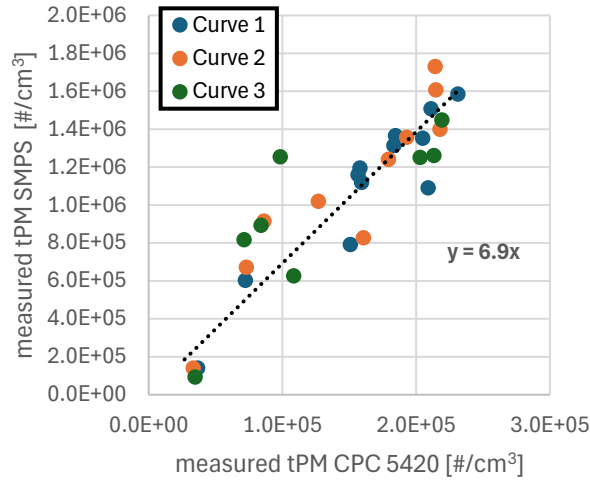


Figure 27: PM number measured by the Grimm 5420 CPC behind the eDiluter™ 2nd stage plotted against the total number from the TSI SMPS behind the eDiluter™ 1st stage while sampling PW127G exhaust

The measured GMD and PSD from the SMPS are presented in Figure 28, which shows an increase in size from ground idle to ~30% shaft power, and then similar PSDs shapes at varying amplitudes, with a GMD around 57 nm and a GSD around 1.78 at the higher shaft powers. This finding is maybe in agreement with the CO₂ emissions presented earlier (Figure 25), which suggested that the combustor AFR was remaining somewhat stable at higher powers.

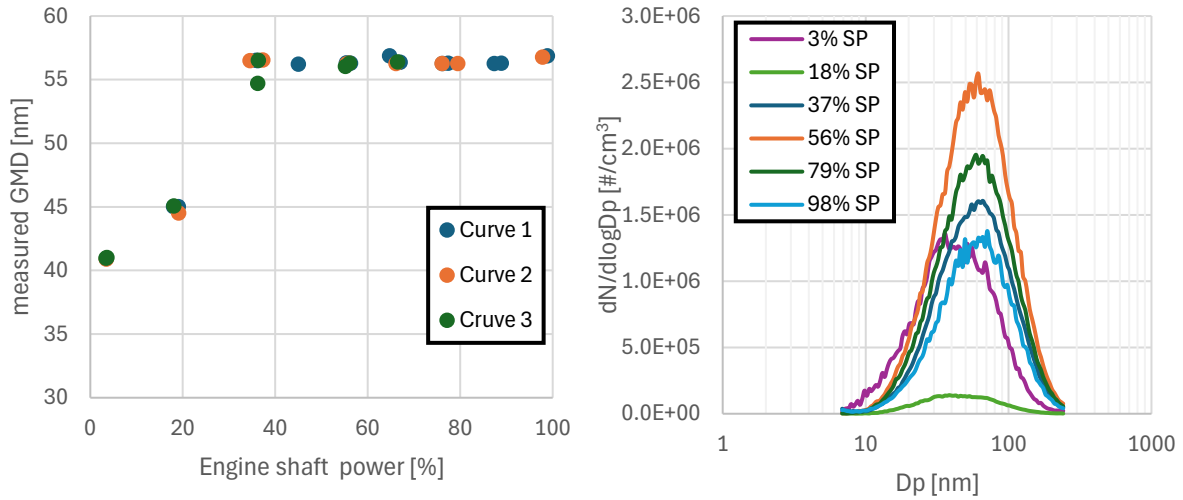


Figure 28: Geometric Mean Diameter (left) and Particle Size distribution (right) measured by the SMPS at different engine power conditions while sampling PW127G exhaust

The total EI number emissions, calculated and corrected to STP as described in section 3.1.3, are shown in Figure 29 for both the SMPS and CPC. EIs from both instruments display the same trend, with maximum emissions at low idle, decreasing sharply at flight idle and then a slight bell curve as shaft power increases. Overall total EI number ranges from about $1\text{E}15$ up to $7\text{E}15$ particles/kg_{fuel}, similar to the reported EI number emissions for another turboprop engine reported in the literature [14] and within the range of regulatory nvPM EI emissions from the ICAO emission databank [10].

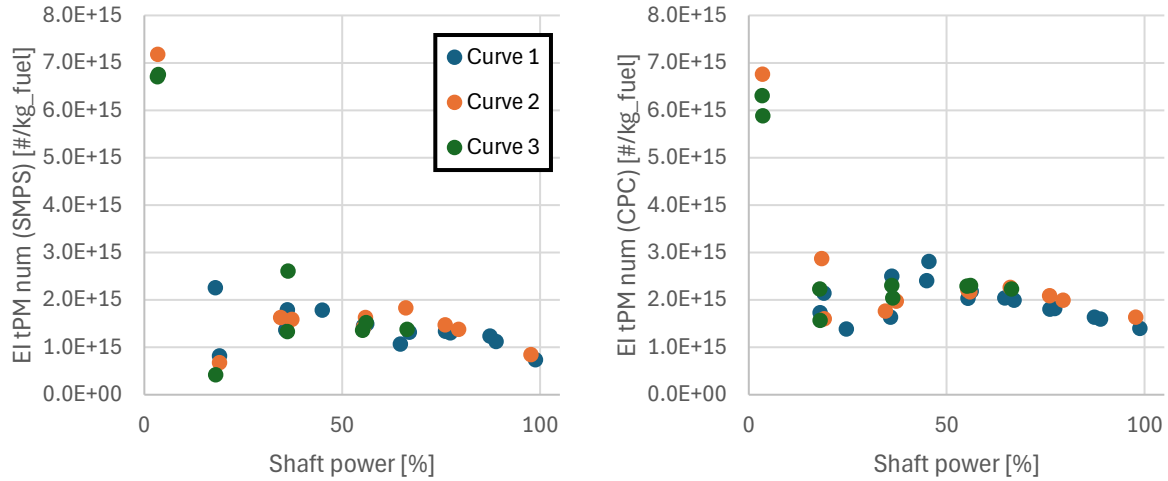


Figure 29: total PM EI number derived from the SMPS (left) and from the CPC (right)

PM EI mass was also derived from the SMPS PSD measurement. The number-space PSD was converted into mass-space assuming an average particle effective density of 1.03 g/cm^3 . This density was calculated using the fit from Durdina et al. [13] and minimising the N/M ratio. Given the maximum measured particle size achievable by the SMPS configuration used was 241.4 nm, and therefore didn't capture the full volume-space PSD, a single lognormal fit was used to derive the volume-space based PSD and hence derive the total mass.

The resultant PM EI mass, reported in Figure 30, exhibits a similar behaviour to PM EI number, with a maximum at ground idle, and then a more pronounced bell shape with increasing shaft power. The SMPS-derived EI mass ranged from approximately 90 up to 1300 mg/kg of fuel, a relatively high value when compared to modern turbofan data which typically report nvPM EI mass' ranging between 0.6 to 292 mg/kg of fuel [15], [16], [17], [18], [19], [20], [21]. However, it is noted that these derived EI mass' are in generally in agreement with reported EI mass emissions for less efficient turboprop (~1500-4000 mg/kg of fuel [14]), turboshaft (~200-600 mg/kg of fuel [9]), and APU (~100-800 mg/kg of fuel [3]) engines.

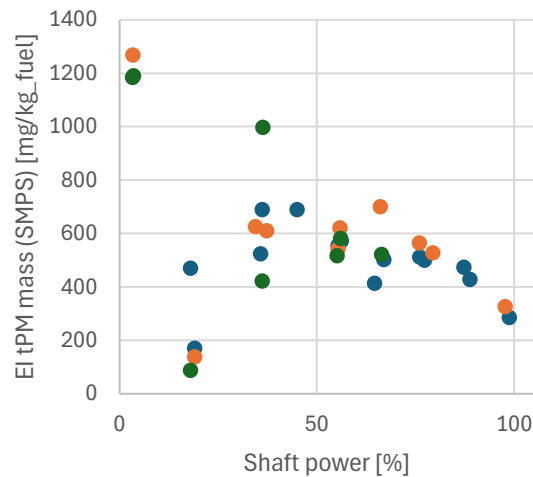


Figure 30: PM EI mass derived from the SMPS

3.2.3. Non-volatile PM emissions

nvPM EI number emissions, calculated from the CPC with additional catalytic stripper (CS), following correction to STP (as described in section 3.1.3) and size dependant loss correction through the CS, are presented in Figure 31 (a). The nvPM EI number is seen to steadily decrease with increasing power and ranged from $7\text{E}13$ to $2.5\text{E}15$ particles/kg of fuel. It is noted that these values are relatively low when compared with the literature (turboprop $\sim 3\text{E}15$ to $11\text{E}15$ particles/kg of fuel [14], turboshaft $\sim 3\text{E}15$ to $7\text{E}15$ particles/kg of fuel [9]), and APU $\sim 2\text{E}15$ to $7\text{E}15$ particles/kg of fuel [3]), suggesting that either the nvPM CS-CPC was malfunctioning or that the measured engine-exit emissions constituted a high fraction of volatile PM (e.g., oil).

This is further substantiated by the tPM/nvPM ratio ranging from ~ 4 to 28 (Figure 31 (b)). The tPM to nvPM difference is further depicted in the timeseries plot in Figure 32, showing both CPCs responding at the same time to changes in the sampled aerosol, with a larger difference at high shaft power and a smaller difference at the lowest shaft power.

It should be noted that following this observation additional post-test laboratory testing was undertaken comparing the nvPM CS-CPC to the tPM CPC and the EUR nvPM reference system on a range of laboratory-generated proxy particles to check the CS-CPCs functionality. The conclusion of this additional testing was that the CS-CPC was working as expected, with a tPM/nvPM ratio of <1.3 when sampling nebulised aircraft soot, likely stemming from uncertainty in the CPC counting efficiency and CS loss correction.

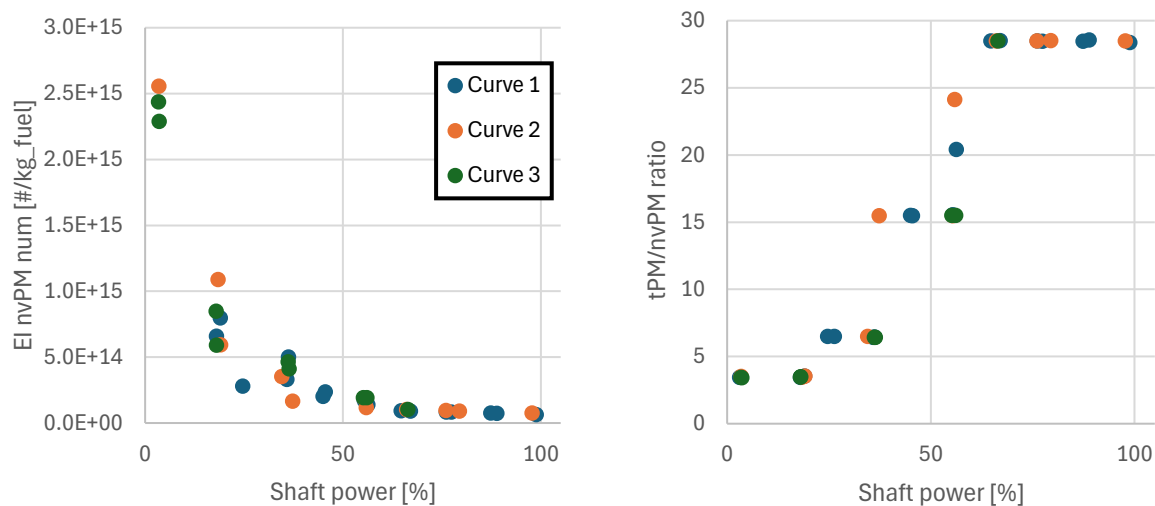


Figure 31: nvPM EI number (left) and total PM to nvPM ratio (right) against shaft power

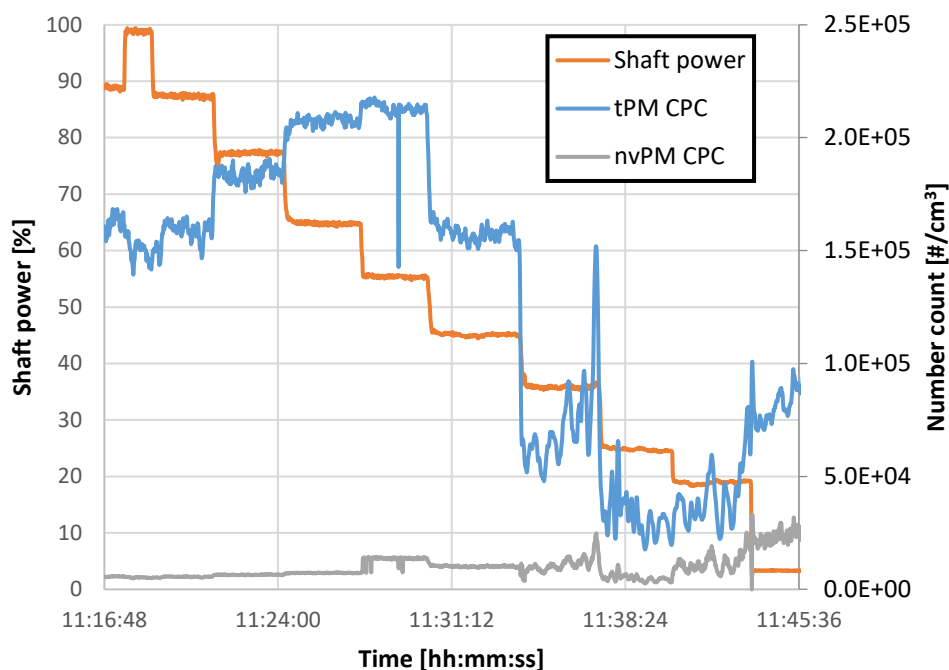


Figure 32: Timeseries showing the shaft power (orange – left y-axis) and total and non-volatile PM CPCs measurements (blue and grey – right y-axis)

Unfortunately, no nvPM EI mass emissions are reported, as the LII-300 didn't measure any signal during the engine emissions test. The sample flow rate was checked prior to the test, and the manufacturer (Artium) confirmed that there were no indications of an issue in the signals, laser fluence, or other operational parameters. Small changes of internal temperatures and pressures within the instrument may indicate that there was a change in sample flow through the instrument during the test. The absence of a measured nvPM mass likely suggests that no sample was reaching the LII-300 sample cell. However, other theories could explain this result such as the emissions being composed of volatiles/organics, which are not measured by laser induced incandescence.

To investigate this further, during an additional laboratory trial following the engine test, the INTA LII-300 was compared against both the LII-300 and MSS from the EUR nvPM reference system. The comparison demonstrated good agreement on nebulised carbon black and nebulised aircraft soot within a concentration range of approximately 30–2000 $\mu\text{g}/\text{m}^3$. However, it is noted that during this laboratory testing, the INTA LII-300 sampling was controlled by a mass-flow controller and vacuum pump, whereas during the PW127G test, sampling was controlled by an eductor pump as is typically employed by INTA. Given that the LII-300 was operating at ~ 900 mbar in parallel with instruments equipped with strong vacuum pumps during the PW127G tests, it is hypothesised that the eductor pump was unable to draw a sample from the splitter with the stronger pumps, resulting in the LII-300 not sampling any flow.

4. Summary of nvPM emissions from small and non-regulated engines

The nvPM emissions from the LF507 and ALF502 as measured with a ICAO A16V2 compliant system, along with PM emissions from a PW127G measured using a 'novel' sampling and measurement system are compared with data from three additional non-regulated turbofan engines, measured by the Swiss (SMARTEMIS) nvPM reference system in previous test campaigns, namely a Honeywell TFE731-60 [21], a FJ44-4, and a PW545A¹¹, are compared in this section against the regulatory limits set by ICAO for the nvPM emissions of gas turbine engines >26.7 kN.

4.1. ICAO nvPM regulatory levels

The nvPM mass and nvPM number emitted during the reference LTO cycle are shown in Figure 33 for the six different engines, along with the regulatory limits set by ICAO for in production and new gas turbine engines.

The PW127G is a turboshaft engine and is rated in terms shaft horsepower (SHP) rather than thrust as is the case for turbofan engines. To enable comparison of the PM emissions from the PW127G with that of the other small/non-regulated engines, its maximum mechanical power output (2130 SHP) was converted to maximum rated thrust in kN. To facilitate this a number of assumptions were required including assuming a propeller efficiency of 0.85 and a take-off airspeed of approximately 100 m/s. To approximate an equivalent thrust rating the following steps were then applied.

- 1) Convert maximum power from SHP to Watts: 1 SHP = 745.7 Watts so Power = 2130 x 745.7
- 2) Convert maximum power to effective power: Power = 2130 x 745.7 x 0.85
- 3) Divide by airspeed to get thrust: Thrust (N) = Effective power (W) / Airspeed (m/s) = 13.5 kN

It is noted that this calculation is only undertaken to allow the data from the PW127G turboprop engine to be plotted at a rough equivalent thrust rating, as would be reported for a turbofan. As such its accuracy is not important but allows an indicative rating of the turboprop compared to a turbofan.

The equivalent LTO points also had to be assumed for the PW127G, with flight idle (7%) assumed to correspond with 18% shaft power, approach (30%) corresponding to 36% shaft power, climb (85%) corresponding to 80% shaft power, and take-off (100%) corresponding to the maximum shaft power. Given it remains unclear as to the discrepancy between PM EI number derived from either the SMPS/ CPC and the CS-CPC (nvPM) from the PW127G, the PM emissions during the LTO cycle are reported both in terms of PM and nvPM for this engine.

Overall, Figure 33 shows that all small and non-regulated engines emit nvPM emissions significantly lower than the current limit for in production engines at equivalent thrusts, with only the PW127G (tPM) and PW545A emitting above the lower limit for new type engines.

¹¹ (Durdina et al. 2025 submitted to ES&T Air)

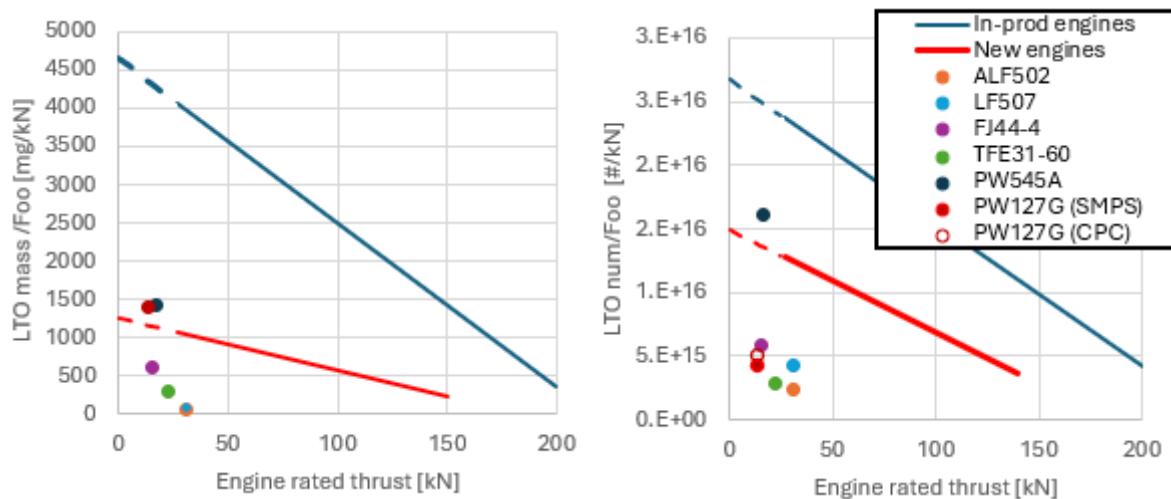


Figure 33: nvPM mass (left) and number (right) emitted during the reference LTO for various small and non-regulated engines

Similarly, the maximum nvPM mass for all engines is significantly lower than the ICAO limit, as can be seen in Figure 34.

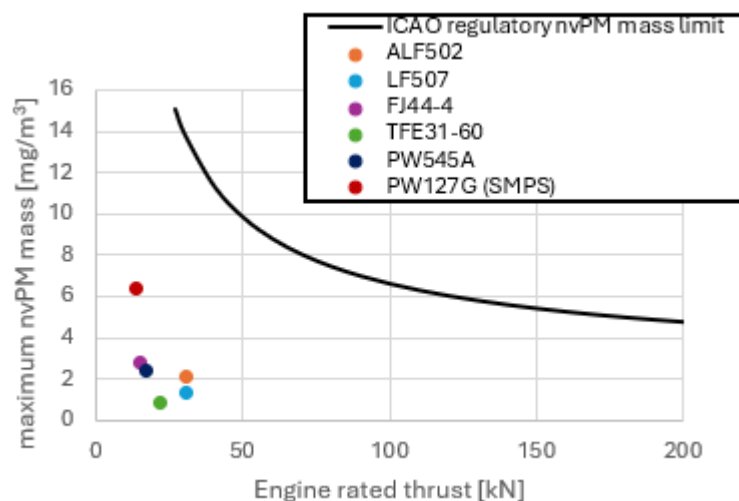


Figure 34: Maximum nvPM mass (measured $\times k_{thermo} \times DF_1$) for various small and non-regulated engines

4.2. N/M Vs GMD

As a comparison of nvPM emissions between regulated and non-regulated engines, the nvPM number to mass ratio (N/M) for the six engines were also correlated with the engine exit GMD affording comparison against a fit from Durdina et al. [13], derived from 42 engines across 19 turbofan types.

As shown in Figure 35, small and non-regulated engines exhibit a wide range of GMDs (approximately 10 nm to 55 nm). All data falls within the 95% confidence bounds (dashed line) from the Durdina et al. fit, except for the PW127G at >30% shaft power.

Generally, given similarity in PM produced in gas turbine engines the GMD is expected to correlate with the N/M ratio, and deviations from the fit are indicative of changes in particle morphology. For example, more agglomerated (i.e., structures with lower fractal dimension and more chain-like formations) can have a larger GMD without a significant change in mass.

This suggests that the PM emissions from the PW127G >30% shaft power maybe less dense or more loosely packed than typical aircraft exhaust nvPM, or that the measurement uncertainty of the utilised SMPS may have resulted in an overestimation of the GMD at these higher powers.

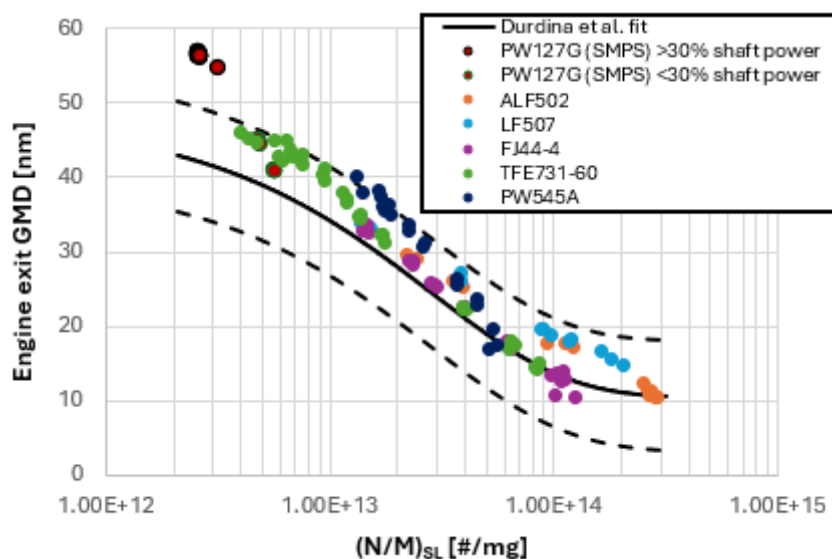


Figure 35: Engine exit plane nvPM GMD as a function of the ratio of regulatory system loss (SL) corrected nvPM number to mass (N/M) with Durdina et al. fit [13] (dashed lines represent 95% confidence intervals)

ACKNOWLEDGEMENTS

The SAMPLE IV consortium wish to express their gratitude to the Natural Environmental Research Council (NERC) and the National Centre for Atmospheric Science (NCAS) for their support and funds from the UKRI Decarbonisation Initiative, which facilitated the Hawarden engine testing reported in the SAMPLE IV Deliverables 3, 5, 6 & 7. Likewise, a special thanks to the Swiss Federal Office of Civil Aviation (FOCA), for the funding of the three emission tests of the non-regulated engines conducted using the Swiss nvPM reference system.

REFERENCES

- [1] ICAO, 'Annex 16 - Environmental Protection - Volume II - Aircraft Engine Emissions', Fifth edition, Jul. 2023. Accessed: May 08, 2024. [Online]. Available: <https://store.icao.int/en/annex-16-environmental-protection-volume-ii-aircraft-engine-emissions>
- [2] P. Lobo *et al.*, 'Comparison of standardized sampling and measurement reference systems for aircraft engine non-volatile particulate matter emissions', *J. Aerosol Sci.*, p. 105557, Mar. 2020, doi: 10.1016/j.jaerosci.2020.105557.
- [3] E. Durand, P. Lobo, A. Crayford, Y. Sevcenco, and S. Christie, 'Impact of fuel hydrogen content on non-volatile particulate matter emitted from an aircraft auxiliary power unit measured with standardised reference systems', *Fuel*, vol. 287, p. 119637, Mar. 2021, doi: 10.1016/j.fuel.2020.119637.
- [4] J. Harper, 'An Experimental Study of the nvPM Emissions Produced by Alternative Aviation Fuels in a Newly-Developed RQL Research Combustor', Thesis (PhD), Cardiff University, 2022.
- [5] SAE international, 'ARP 1179D - Aircraft Gas Turbine Engine Exhaust Smoke Measurement', SAE International, 2011. doi: 10.4271/ARP1179D.
- [6] 'ARP6481A: Procedure for the Calculation of Non-Volatile Particulate Matter Sampling and Measurement System Losses and System Loss Correction Factors - SAE International'. Accessed: Dec. 05, 2024. [Online]. Available: <https://www.sae.org/standards/content/arp6481a/>
- [7] 'ARP1533C - Procedure for the Analysis and Evaluation of Gaseous Emissions from Aircraft Engines'.
- [8] SAE International, 'ARP 6320B - Procedure for the Continuous Sampling and Measurement of Non-Volatile Particulate Matter Emissions from Aircraft Turbine Engines', 2024, doi: <https://doi.org/10.4271/ARP6320>.
- [9] M. Rohkamp *et al.*, 'Gaseous and particulate matter (PM) emissions from a turboshaft-engine using different blends of sustainable aviation fuel (SAF)', *Aerosol Sci. Technol.*, vol. 0, no. 0, pp. 1–16, 2024, doi: 10.1080/02786826.2024.2417977.
- [10] 'ICAO Aircraft Engine Emissions Databank', EASA. Accessed: Mar. 07, 2019. [Online]. Available: <https://www.easa.europa.eu/easa-and-you/environment/icao-aircraft-engine-emissions-databank>
- [11] L. Durdina, B. T. Brem, M. Elser, D. Schönenberger, F. Siegerist, and J. G. Anet, 'Reduction of Nonvolatile Particulate Matter Emissions of a Commercial Turbofan Engine at the Ground Level from the Use of a Sustainable Aviation Fuel Blend', *Environ. Sci. Technol.*, vol. 55, no. 21, pp. 14576–14585, Nov. 2021, doi: 10.1021/acs.est.1c04744.
- [12] E. Durand *et al.*, 'Correction for particle loss in a regulatory aviation nvPM emissions system using measured particle size', *J. Aerosol Sci.*, vol. 169, p. 106140, Mar. 2023, doi: 10.1016/j.jaerosci.2023.106140.
- [13] L. Durdina *et al.*, 'Characterizing and Predicting nvPM Size Distributions for Aviation Emission Inventories and Environmental Impact', *Environ. Sci. Technol.*, vol. 58, no. 24, pp. 10548–10557, Jun. 2024, doi: 10.1021/acs.est.4c02538.
- [14] E. Corporan, A. Quick, and M. J. DeWitt, 'Characterization of Particulate Matter and Gaseous Emissions of a C-130H Aircraft', *J. Air Waste Manag. Assoc.*, vol. 58, no. 4, pp. 474–483, Apr. 2008, doi: 10.3155/1047-3289.58.4.474.
- [15] E. Durand, 'Towards improved correction methodology for regulatory aircraft engine nvPM measurement', Thesis (PhD), Cardiff University, 2019. Accessed: Jan. 28, 2020. [Online]. Available: <http://orca.cf.ac.uk/126400/>
- [16] P. Lobo, D. E. Hagen, P. D. Whitefield, and D. Raper, 'PM emissions measurements of in-service commercial aircraft engines during the Delta-Atlanta Hartsfield Study', *Atmos. Environ.*, vol. 104, pp. 237–245, Mar. 2015, doi: 10.1016/j.atmosenv.2015.01.020.
- [17] A. M. Boies *et al.*, 'Particle Emission Characteristics of a Gas Turbine with a Double Annular Combustor', *Aerosol Sci. Technol.*, vol. 49, no. 9, pp. 842–855, Sep. 2015, doi: 10.1080/02786826.2015.1078452.
- [18] P. Lobo *et al.*, 'Measurement of Aircraft Engine Non-Volatile PM Emissions: Results of the Aviation-Particle Regulatory Instrumentation Demonstration Experiment (A-PRIDE) 4 Campaign', *Aerosol Sci. Technol.*, vol. 49, no. 7, pp. 472–484, Jul. 2015, doi: 10.1080/02786826.2015.1047012.

- [19] D. Delhay *et al.*, 'The MERMOSE project: Characterization of particulate matter emissions of a commercial aircraft engine', *J. Aerosol Sci.*, vol. 105, pp. 48–63, Mar. 2017, doi: 10.1016/j.jaerosci.2016.11.018.
- [20] J. S. Kinsey, M. D. Hays, Y. Dong, D. C. Williams, and R. Logan, 'Chemical Characterization of the Fine Particle Emissions from Commercial Aircraft Engines during the Aircraft Particle Emissions eXperiment (APEX) 1 to 3', *Environ. Sci. Technol.*, vol. 45, no. 8, pp. 3415–3421, Apr. 2011, doi: 10.1021/es103880d.
- [21] L. Durdina, B. T. Brem, D. Schönenberger, F. Siegerist, J. G. Anet, and T. Rindlisbacher, 'Non-Volatile Particulate Matter Emissions of a Business Jet Measured at Ground Level and Estimated for Cruising Altitudes', *Environ. Sci. Technol.*, Oct. 2019, doi: 10.1021/acs.est.9b02513.

APPENDIX

AVL MSS calibration certificate

Calibration Protocol Annual Calibration

Micro Soot Sensor AVL 483 S/N 273

| | |
|------------|-------------------------|
| Instrument | Measuring unit complete |
| Serial No. | 273 |



| | |
|-----------------------|-----|
| Aviation mode active? | YES |
|-----------------------|-----|

| Calibration data | | | | |
|-----------------------|---------|------------|------------------------------------|-----------|
| Calibration factor | | | Zero drift | Rise time |
| old f. cal | f. corr | new f. cal | $\mu\text{g}/\text{m}^3/\text{hr}$ | sec |
| 0,600 | 1,046 | 0,628 | 0,2092 | 0,3 |
| Reference phase angle | | | Reference value span check | |
| old phase | | new phase | old | new |
| -60 | | -59 | 3,780 | 3,748 |

| MW (mg/m ³) 60 sec begin | MW (mg/m ³) 60 sec end |
|---|---------------------------------------|
| 0,0001 | 0,0003 |

The calibration was performed according to the requirements from ICAO Annex 16 Vol.II, Appendix 7.

Date 21.02.2023

Signature

Dok.Nr. D00090245

Seite / page 1 von 4

50000681 / 01

Calibration Protocol Annual Calibration

Micro Soot Sensor AVL 483 S/N 273

| Test No | Nominal EC conc. 0°C ($\mu\text{g}/\text{m}^3$) | OC CONC. 20°C ($\mu\text{g}/\text{m}^3$) | EC CONC. 20°C ($\mu\text{g}/\text{m}^3$) | EC MASS (μg) | % EC | EC mass ($\mu\text{g}/\text{m}^2$) | EC conc. 0°C ($\mu\text{g}/\text{m}^3$) | Deviation from nominal % | MSS soot conc. 0°C ($\mu\text{g}/\text{m}^3$) | MSS soot conc. 0°C (mg/m^3) |
|---------|---|---|---|------------------------------|-------|---|---|-----------------------------|---|---|
| 0 001 | 0 | | | | | | 0,0 | | 0,1 | 0,0001 |
| 0 002 | | | | | | | 0,0 | | 0,1 | 0,0001 |
| 0 003 | | | | | | | 0,0 | | -0,2 | -0,0002 |
| 100 BG | 100 | 28,1 | | | | | | | 100,8 | 0,1008 |
| 100 001 | | 27,6 | 101,9 | 17,3 | 100,5 | 13,2 | 109,4 | 9,4 | 101,6 | 0,1016 |
| 100 002 | | 32,1 | 103,9 | 17,5 | 96,3 | 13,4 | 111,5 | 11,5 | 100,5 | 0,1005 |
| 100 003 | | 38,9 | 101,0 | 17,1 | 90,4 | 13,1 | 108,4 | 8,4 | 101,4 | 0,1014 |
| 250 BG | 250 | 45,7 | | | | | | | 246,7 | 0,2467 |
| 250 001 | | 50,1 | 245,9 | 16,4 | 98,2 | 12,5 | 263,9 | 5,6 | 243,3 | 0,2433 |
| 250 002 | | 48,2 | 257,5 | 17,2 | 99,1 | 13,1 | 276,3 | 10,5 | 259,4 | 0,2594 |
| 250 003 | | 50,5 | 245,1 | 16,4 | 98,1 | 12,5 | 263,1 | 5,2 | 246,1 | 0,2461 |
| 500 BG | 500 | 59,3 | | | | | | | 563,9 | 0,5639 |
| 500 001 | | 68,9 | 549,4 | 18,1 | 98,3 | 13,8 | 589,6 | 17,9 | 565,3 | 0,5653 |
| 500 002 | | 72,5 | 508,7 | 16,8 | 97,5 | 12,8 | 546,0 | 9,2 | 515,2 | 0,5152 |
| 500 003 | | 69,6 | 567,6 | 18,7 | 98,2 | 14,3 | 609,2 | 21,8 | 583,6 | 0,5836 |

Dok.Nr. D00090245

Seite / page 3 von 4

50000681 / 01

AVL APC calibration certificate (VPR+CPC)

AVL 489 Particle Counter Aviation Calibration Certificate

| |
|---------------------|
| Date: 28-Feb-2023 |
| Device: GH0672 382C |
| Chopper Diluter 460 |

| | | |
|-------|--------|-------|
| Makro | XF0339 | V1.31 |
|-------|--------|-------|

| Used Instruments | Type | Serial No. |
|--|-----------------------|---------------|
| DMA | TSI 3082 | 3082001514002 |
| Master CPC | TSI 3792 | 3792151801 |
| Mass Flow Meter | Vögtlin GCR-B5SA-BA25 | 139898 |
| Calibration aerosol: APG combustion soot | | |

| Measured Inlet Flows of Instruments | | |
|-------------------------------------|-------------|---------------------|
| Device | Vol. Flow | Normalization Cond. |
| APC Chopper Dil. low | 4736 ml/min | 25°C; 1013.25mbar |
| Master CPC | 1022 ml/min | ambient conditons |

| Zero Concentration with HEPA-Filter | | |
|-------------------------------------|-------------|-------------------|
| APC | 0.29 #/cm³ | at pcrf=10*10=100 |
| Master CPC | 0.013 #/cm³ | |



| Nr | Diluter 1 low/high | values set | | set pcrf | Flows Dilution Factor | Measured Penetrations | | | |
|----|-----------------------|------------|-----------|-------------|--------------------------|-----------------------|----------------|----------------|----------------|
| | | Diluter 1 | Diluter 2 | | | 100nm (>70%) | 50nm (>65%) | 30nm (>55%) | 15nm (>30%) |
| 1 | low | 10 | 10 | 100 | 69 | 71.3% | 70.1% | 66.6% | 48.7% |
| 2 | low | 25 | 10 | 250 | 176 | 74.5% | 71.4% | 66.3% | 46.3% |
| 3 | low | 50 | 10 | 500 | 360 | 76.1% | 73.6% | 66.7% | 47.3% |
| 4 | low | 100 | 10 | 1000 | 728 | 76.2% | 75.9% | 66.4% | 47.3% |
| 5 | low | 150 | 10 | 1500 | 1092 | 80.2% | 73.3% | 65.7% | 45.8% |

*Only calibrated at Stages 1-5. One of those stages MUST be used for ICAO Annex 16: Environmental Protection, Vol. II, Appendix 7 compliant measurements.

| | |
|---|--------|
| Volatile Particle Removal Efficiency for Tetracontane 30nm: | 99.97% |
|---|--------|

AVL List GmbH does hereby certify that the above described instrument conforms to the original manufacturer's specifications and has been calibrated using the standards whose accuracies are traceable to national standards or have been derived from accepted values of natural physical constants or have been derived by the ration type of self calibration techniques. This report may not be reproduced, except in full, unless permission for the publication of an approved abstract is obtained in writing from the calibration organization issuing this report.


Robert Hoefler

Page 1 of 2

| Nr | Flows Dilution Factor | Measured particles dilution | | | |
|----|-----------------------------|-----------------------------|-------|-------|-------|
| | | 100 nm | 50 nm | 30 nm | 15 nm |
| 1 | 69 | 97 | 98 | 104 | 142 |
| 2 | 176 | 236 | 246 | 265 | 379 |
| 3 | 360 | 473 | 489 | 540 | 762 |
| 4 | 728 | 955 | 959 | 1096 | 1538 |
| 5 | 1092 | 1362 | 1490 | 1663 | 2385 |

Calibration values set in firmware

Directly measured values for the seven fixed PCRF settings

| PCRF | calib. value |
|------|--------------|
| 100 | 1.11 |
| 250 | 1.09 |
| 500 | 1.07 |
| 1000 | 1.06 |
| 1500 | 1.06 |

Pressures during calibration

| | |
|------------------------|----------|
| Sample Rel. Pressure | -17 mbar |
| Diluted. Rel. Pressure | 16 mbar |
| Absolute Pressure | 982 mbar |

Demand temperatures during calibration

| | |
|--------------------------|--------|
| Catalytic Stripper Temp. | 350 °C |
| Diluter 1 Temperature | 150 °C |

Specifications of the Catalytic Stripper

| |
|---|
| Oxidation efficiency: >99% for decane inlet concentration of 4% |
| Sulphur Storage Capacity: > 8mg |

* These values are calculated by averaging the values measured at the highest and the lowest Diluter 1 setting for each Diluter 2 setting.

Page 2 of 2

AVL List GmbH
Hans-List-Platz 1
8020 Graz
AUSTRIA



Kalibrierstelle für Durchfluss, Spannung und Strom sowie Partikelanzahlkonzentration
Calibration Body for flow rate, voltage and current, and particle number concentration

akkreditiert durch / accredited by
AKKREDITIERUNG AUSTRIA



| |
|-----------------------------------|
| PN_3876 |
| Akkreditierung Austria 0626 |
| 28-Feb-2023 |

Kalibrierschein nach ISO/IEC17025
Calibration Certificate according to ISO/IEC 17025

Kalibrierzeichen
Calibration Mark

| | | |
|---|--|--|
| Gegenstand <i>Object</i> | Condensation Particle Counter | Dieser Kalibrierschein dokumentiert die Rückführbarkeit auf nationale Normale zur Darstellung der physikalischen Einheiten in Übereinstimmung mit dem Internationalen Einheitensystem (SI). |
| Hersteller <i>Manufacturer</i> | TSI Inc. | |
| Type <i>Type</i> | TSI 3790 | Akkreditierung Austria ist Unterzeichner der multilateralen Übereinkommen der European Co-operation for Accreditation (EA) und der International Laboratory Accreditation Cooperation (ILAC) zur gegenseitigen Anerkennung der Kalibrierscheine. |
| Seriennummer <i>Serial number</i> | 3790132002 | <i>This calibration certificate documents the traceability to national standards, which realize the physical units of measurements according to the International system of Units (SI).</i> |
| Auftraggeber <i>Customer</i> | AVL List GmbH Hans-List-Platz 1 8020 Graz AUSTRIA | <i>Akkreditierung Austria is a signatory to the multilateral agreements of the European Co-operation for Accreditation (EA) and of the International Laboratory Accreditation Cooperation (ILAC) for the mutual recognition of calibration certificates.</i> |
| Kalibriernummer <i>Order No.</i> | PN_3876 | |
| Anzahl der Seiten des Zertifikats <i>Number of pages of the certificate</i> | 5 | |
| Datum der Kalibrierung <i>Date of calibration</i> | 28-Feb-2023 | |

Dieser Kalibrierschein darf nur vollständig und unverändert weiterverbreitet werden. Auszüge oder Änderungen sind unzulässig. Kalibrierscheine ohne Unterschrift und Stempel haben keine Gültigkeit.
This calibration certificate may not be reproduced other than in full. Calibration certificates without signature and seal are not valid.

28-Feb-2023

Bernd Friedl

Georg Aigner

| | | |
|--|---|---|
| Datum <i>Date</i> | Zeichnungsberechtigter <i>Authorised person</i> | Prüfer <i>Tester</i> |
| AVL List GmbH Hans-List-Platz 1, 8020 Graz, Austria Tel.: +43 316 787-0 Fax: +43 316 787-400 Email: info@avl.com, www.avl.com | | AVL List GmbH Hans-List-Platz 1 A-8020 Graz, Austria Phone: +43 316 787-0 www.avl.com |

Firmenbuchnummer: FN 53507M
Landes- als Handelsgericht Graz
UID-Nr: ATU28752908

| |
|-----------------------------|
| PN_3876 |
| Akkreditierung Austria 0626 |
| 28-Feb-2023 |

Seite 2/5 zum Kalibrierschein vom 28-Feb-2023
Page 2/5 of calibration certificate dated 28-Feb-2023



Kalibriergegenstand
Unit under test

Das vorliegende Gerät mit der Type TSI 3790 und der Seriennummer 3790132002 ist Gegenstand der Kalibrierung. Die Ergebnisse beziehen sich ausschließlich auf den bezeichneten Gegenstand zum Zeitpunkt der Kalibrierung.
The present measurement device of the type TSI 3790 and the serial number 3790132002 will be calibrated. The results refer only to the object designated at the time of calibration.

Eingestellte interne Parameter vor der Kalibrierung:
Preset internal parameters prior to calibration

| | | | |
|---|---------|---|------|
| Saturatortemperatur <i>Saturator Temperature</i> | 39.0 °C | Firmware Version <i>Volumetric Inlet flow rate</i> | 2.31 |
| Kondensortemperatur <i>Condenser Temperature</i> | 20.0 °C | | |
| Optiktemperatur <i>Optics Temperature</i> | 40.0 °C | | |

Kalibrierort
Site of calibration

AVL - Kalibrierlabor Babenbergerstraße
Babenbergerstraße 88
A-8020 Graz

Kalibrierverfahren
Calibration procedure

Kalibrierung - Partikelanzahlkonzentration
Calibration - Particle Number Concentration

Die Kalibrierung der Partikelanzahlkonzentration des Kondensationspartikelzählers erfolgt nach ISO 27891:2015 mit einem Aerosolelektrometer als Referenzgerät. Die Berechnung der Zählleistung erfolgt nach Kapitel D.2.4 von ISO 27891:2015.
The calibration of the particle number concentration of the condensation particle counter is performed according to ISO 27891:2015 using an aerosol electrometer as reference instrument. The method used to calculate the detection efficiency is described in chapter D.2.4 of ISO 27891:2015.

| | |
|---|------------------------------|
| Verwendete Kalibriervorschrift <i>Used calibration instruction</i> | D00811149 / 05 |
| Verfahrensbeschreibung <i>Used process instruction</i> | D00855277 / 01 14.12.2021 |
| Verwendete Kalibriersoftware <i>Used calibration software</i> | XF0713 Version: V1.10 |

Messbedingungen
Measurement conditions

Es werden mit einem Elektrospray-Aerosolgenerator Emery Oil Nanopartikel in einem Luft-CO₂-Gemisch (1,4 l/min Luft, 0,1 l/min CO₂) erzeugt, diese werden mittels elektrischer Mobilitätsklassifizierung mit einem DEMC klassifiziert. Bei dem Referenz-aerosolelektrometer wird ein volumetrischer Einlassfluss von 1 l/min eingestellt. Es wird keine Mehrfachladungskorrektur angewandt, da die Größenverteilung des Primäraerosols hinreichend schmal ist (Mehrfachladungsanteil <0,1%).
An electrospray aerosol generator is used to generate Emery Oil nanoparticles within an air-CO₂ mixture (1,4 l/min air, 0,1 l/min CO₂). These particles are classified according to electrical mobility with a DEMC. The reference aerosol electrometer has a set volumetric flow of 1 l/min. No multiple charge correction is applied since the width of the primary aerosol distribution is deemed sufficiently narrow (Multiple charge fraction <0,1%).

AVL List GmbH
Hans-List-Platz 1, 8020 Graz, Austria
Tel.: +43 316 787-0 Fax: +43 316 787-400
Email: info@avl.com, www.avl.com

Firmenbuchnummer: FN 53507M
Landes- als Handelsgericht Graz
UID-Nr: ATU28752908

Umgebungsbedingungen Ambient conditions

Raumtemperatur:
Room temperature
Relative Luftfeuchte:
Relative humidity
Barometrischer Luftdruck:
Barometric pressure

| Gem. Wert Measured val. | Untergrenze Lower limit | Obergrenze Upper limit |
|----------------------------|----------------------------|---------------------------|
| 22.0 °C | 20.0 °C | 26.0 °C |
| 49% | 20% | 60% |
| 982 hPa | N/A | N/A |

Verwendete Referenzgeräte Reference equipment used

| Messgröße / Measurement parameter | Type | Hersteller Manufacturer | Seriennummer Serial number |
|---|-------------------|----------------------------|-------------------------------|
| Raumtemperatur / Ambient Temperature | Almemo FHAD46-C2 | Ahlborn | H20090670/20090190 |
| Luftfeuchte / Ambient Humidity | Almemo FHAD46-C2 | Ahlborn | H20090670/20090190 |
| Luftdruck / Ambient Pressure | Almemo FHAD46-C2 | Ahlborn | H20090670/20090190 |
| Volumetrischer Einlassfluss / Volumetric Flow rate | Caltrak SL-800-24 | Sierra | 157787 |
| Aerosolfeuchte / Aerosol Humidity | HM42 | Vaisala | P2530244 |
| Aerosoldruck / Aerosol Pressure | Almemo FDA612SR | Ahlborn | H20090670/20010008 |
| Elektrischer Mobilitätsdurchmesser - Klassifizierer Electrical Mobility Diameter - Classifier | 3082 | TSI | 3082001701001 |
| Elektrischer Mobilitätsdurchmesser - DMA-Säule Electrical Mobility Diameter - DMA | 3085 | TSI | 3085A1653001 |
| Partikelanzahlkonzentration / Particle Number Concentration Certificate/Zertifikat: 212-08213 | 3068b | TSI | 3068161201 |

Messunsicherheit Measurement uncertainty

Angegeben ist die erweiterte Messunsicherheit, die sich aus der Standardunsicherheit durch die Multiplikation mit dem Erweiterungsfaktor $k=2$ ergibt. Sie wurde für die Partikelanzahlkonzentration gemäß ISO27891:2015 ermittelt. Der Wert der Messgröße liegt mit einer Wahrscheinlichkeit von annähernd 95% im zugeordneten Werteintervall.
The reported measurement uncertainty of the measurement is stated as the standard uncertainty of measurement multiplied by a coverage factor $k=2$. It has been determined in accordance with ISO27891:2015 for the particle number concentration. The true value is located in the corresponding interval with a probability of 95%.

Wiederholung der Kalibrierung Interval of recalibration

Für die Einhaltung einer angemessenen Frist zur Wiederholung der Kalibrierung ist der Benutzer verantwortlich. Für Abgastests nach UN/ECE R83 Rev. 5 oder UN/ECE R49 Rev. 6 ist eine Kalibrierung innerhalb von 12 Monaten vor dem Test notwendig.
The user is responsible to have the object recalibrated at appropriate intervals. For emissions tests according to UN/ECE R83 Rev. 5 or UN/ECE R49 Rev. 6 a calibration is necessary within a 12 month period prior to the test.

AVL List GmbH
Hans-List-Platz 1, 8020 Graz, Austria
Tel. +43 316 287-0 Fax +43 316 287-400
Email: info@avi.com, www.avi.com

Firmenbuchnummer: FN 33507M
Landes- als Handelsgericht Graz
UID-Nr: ATU28752908

Messergebnisse Measurement results

Kalibrierung - Nullpunktüberprüfung Calibration - Zero Check

Messdauer
Sampling duration 15 min

Partikelanzahlkonzentration
Particle number concentration 0.06 #/cm³

Dokumentation von weiteren Messgrößen Documentation of further measured values

Relativdruck Kalibrieraerosol
Relative pressure calibration aerosol -1 hPa

Relative Feuchte Kalibrieraerosol
Relative humidity calibration aerosol 1.6%

Kalibrierung - CPC Einlassfluss Calibration - CPC Inlet flow

| Sollwert Setpoint | Referenzwert Reference value | Abweichung Deviation | Messunsicherheit Meas. Uncertainty | Grenzwert** Limit** | Status |
|-----------------------|---------------------------------|-------------------------|---------------------------------------|------------------------|--------|
| Volumetric [l/min] | Volumetric [l/min] | Normalized* [μm] | [%] | [%] | [] |
| 1.000 | 0.986 | 0.885 | 1.4% | 0.4% | 5% |

*Normalisierungsbedingungen: 0°C, 1013mbar
*Normalization conditions: 0°C, 1013mbar

**Grenzwert entsprechend UN/ECE R83 Rev. 5 und UN/ECE R49 Rev. 6
**Limit according to UN/ECE R83 Rev. 5 and UN/ECE R49 Rev. 6

Zusatzinformation - Druckabfall CPC-Einlass zu Optik 6 mbar
Additional information - Pressure drop CPC inlet to optics

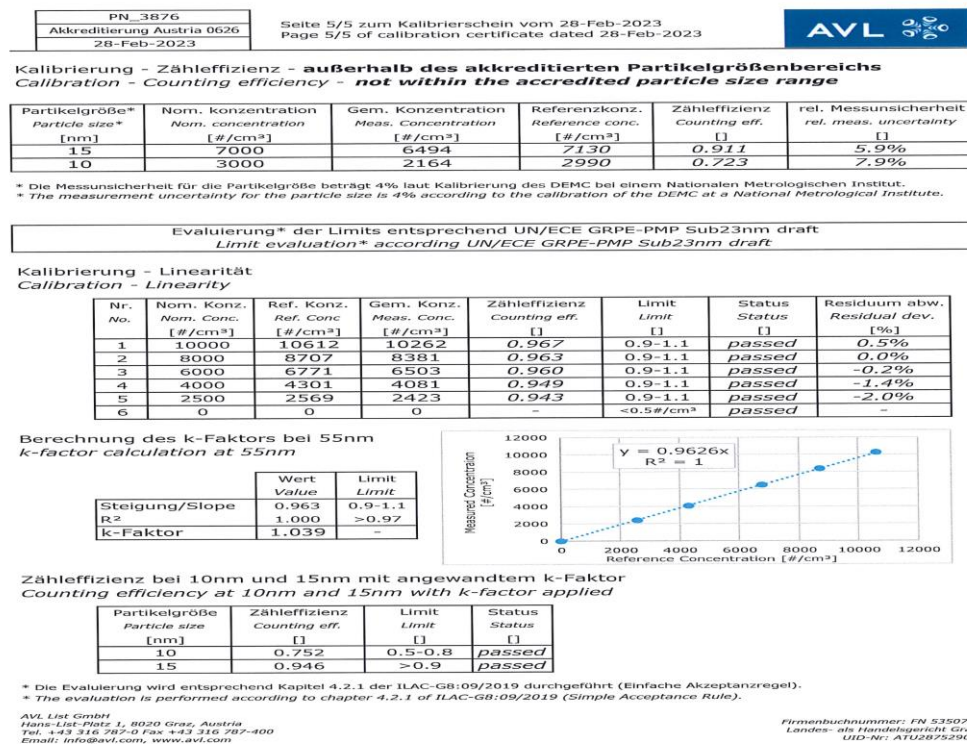
Kalibrierung - Zählereffizienz Calibration - Counting efficiency

| Partikelgröße* Particle size* | Nom. Konzentration Nom. concentration | Gem. Konzentration Meas. concentration | Referenzkonz. Reference conc. | Zähleffizienz Counting eff. | rel. Messunsicherheit rel. meas. uncertainty |
|----------------------------------|--|---|----------------------------------|--------------------------------|---|
| [nm] | [#/cm ³] | [#/cm ³] | [#/cm ³] | [] | [] |
| 55 | 10000 | 10262 | 10612 | 0.967 | 5.9% |
| 55 | 8000 | 8381 | 8707 | 0.963 | 5.9% |
| 55 | 6000 | 6503 | 6771 | 0.960 | 5.9% |
| 55 | 4000 | 4081 | 4301 | 0.949 | 7.9% |
| 55 | 2500 | 2423 | 2569 | 0.943 | 7.9% |

* Die Messunsicherheit für die Partikelgröße beträgt 4% laut Kalibrierung des DEMC bei einem Nationalen Metrologischen Institut.
* The measurement uncertainty for the particle size is 4% according to the calibration of the DEMC at a National Metrological Institute.

AVL List GmbH
Hans-List-Platz 1, 8020 Graz, Austria
Tel. +43 316 287-0 Fax +43 316 287-400
Email: info@avi.com, www.avi.com

Firmenbuchnummer: FN 33507M
Landes- als Handelsgericht Graz
UID-Nr: ATU28752908



Gas analysers' linearity certificates

Linearity Test Certificate



Signal Group Ltd
Standards House, Doman Road
Camberley, Surrey GU15 3DF UK

Tel: +44 (0)1276 612841
Fax: +44 (0)1276 691302
Web: www.signal-group.com

INSTRUMENTATION

| Instrument Details | Serial No. | Range FS |
|--------------------|------------|----------|
| 4000VM | 14951 | 1000 |

TRACEABILITY

| Gas Divider Details | Serial No. | Calibration Date |
|---------------------|------------|------------------|
| 821s | 9367 | 18.04.2023 |

| Analytical Traceability | | | |
|-------------------------|--------------|----------------|-----------------|
| | Cylinder No. | Gas type | Gas value (ppm) |
| Span Gas Mixture | EA54AYA | N ₂ | 40 |
| Diluent gas | KN27XDK | N ₂ | |

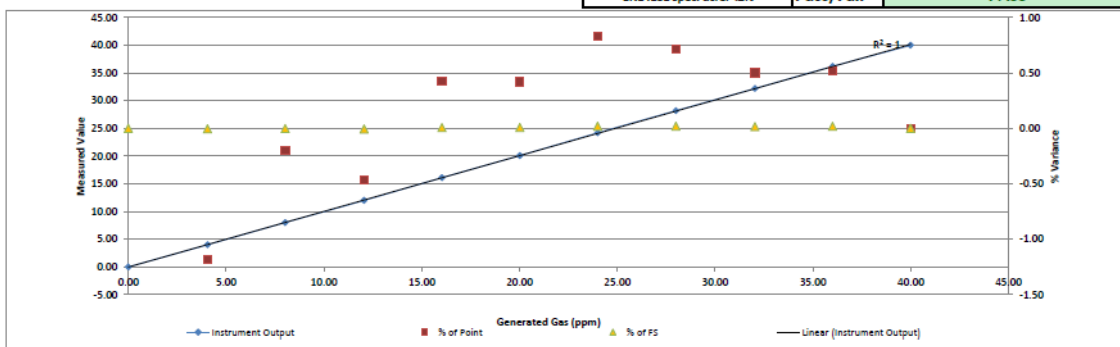
LINEARITY

| Gas Divider Point | Actual | Measured | Regression fit | | | | | | Variance | | |
|-------------------------|--------|----------|----------------|---------|--------------------|-----------|----------------|------------------|------------|----------------|-----------|
| | ppm | ppm | y | (c-c) | (c-c) ² | x*(c-c) | d _e | d _{rel} | (ppm or %) | (% of reading) | (% of FS) |
| 100 | 40.00 | 40.00 | 40.167 | 19.980 | 399.201 | 799.200 | -0.167 | -0.417 | 0.00 | 0.00 | 0.00 |
| 90.03 | 36.01 | 36.20 | 36.160 | 15.992 | 255.744 | 578.911 | -0.149 | -0.372 | 0.19 | 0.52 | 0.02 |
| 80.1 | 32.04 | 32.20 | 32.169 | 12.020 | 144.480 | 387.044 | -0.129 | -0.324 | 0.16 | 0.50 | 0.02 |
| 70 | 28.00 | 28.20 | 28.109 | 7.980 | 63.680 | 225.036 | -0.110 | -0.276 | 0.20 | 0.71 | 0.02 |
| 60 | 24.00 | 24.20 | 24.090 | 3.980 | 15.840 | 96.316 | -0.091 | -0.228 | 0.20 | 0.83 | 0.02 |
| 50.04 | 20.02 | 20.10 | 20.087 | -0.004 | 0.000 | -0.080 | -0.071 | -0.178 | 0.08 | 0.42 | 0.01 |
| 40.08 | 16.03 | 16.10 | 16.084 | -3.988 | 15.904 | -64.207 | -0.052 | -0.130 | 0.07 | 0.42 | 0.01 |
| 30.14 | 12.06 | 12.00 | 12.089 | -7.964 | 63.425 | -95.568 | -0.032 | -0.081 | -0.06 | -0.46 | -0.01 |
| 20.04 | 8.02 | 8.00 | 8.029 | -12.004 | 144.096 | -96.032 | -0.013 | -0.033 | -0.02 | -0.20 | 0.00 |
| 10.12 | 4.05 | 4.00 | 4.042 | -15.972 | 255.105 | -63.888 | 0.006 | 0.015 | -0.05 | -1.19 | 0.00 |
| 0 | 0.00 | 0.00 | -0.025 | -20.020 | 400.800 | 0.000 | 0.025 | 0.063 | 0.00 | | 0.00 |
| Average | 20.02 | 20.09 | Sums (Σ) | 0.000 | 1758.276 | 1766.731 | Average | | 0.07 | 0.16 | 0.01 |
| | | | Slope | | B= | 1.005 | Maximum | | 0.20 | -1.19 | 0.02 |
| | | | Offset | | A= | -0.025 | | | | | |
| EN14181 spec: dcrel <2% | | | | | | Pass/Fail | | PASS | | | |

EN14181 spec: dcrel <2%

Pass/Fail

PASS



Calibrated by: RC

Signed: [Signature]

Date: 10.07.2023

Linearity Test Certificate



Signal Group Ltd
Standards House, Domain Road
Canterbury Surrey GU15 3DF UK

Tel: +44 (0)1276 682841
Fax: +44 (0)1276 691302
Web: www.signal-group.com

INSTRUMENTATION

| Instrument Details | Serial No. | Range FS |
|--------------------|------------|----------|
| 4000VM | 14951 | 1000 |

TRACEABILITY

| Gas Divider Details | Serial No. | Calibration Date |
|---------------------|------------|------------------|
| 821s | 9367 | 18.04.2023 |

| Analytical Traceability | | | | |
|-------------------------|--------------|----------|-----------------|-------------|
| | Cylinder No. | Gas type | Gas value (ppm) | Balance gas |
| Span Gas Mixture | EU80PDZ | NO | 500 | N2 |
| Diluent gas | KN27XDK | N2 | | |

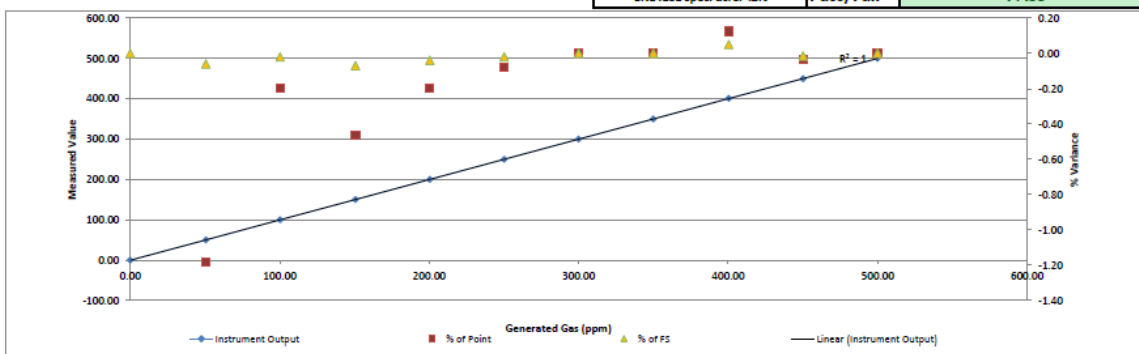
LINEARITY

| Gas Divider Point | Actual | Measured | Regression fit | | | | | | Variance | | |
|-------------------|--------|----------|----------------|----------|--------------------|-----------------------|----------------|--------------------|------------|----------------|-----------|
| | ppm | ppm | y | (c-c) | (c-c) ² | x _i *(c-c) | d _c | d _{c,rel} | (ppm or %) | (% of reading) | (% of FS) |
| 100 | 500.00 | 500.00 | 500.101 | 249.751 | 62375.608 | 124875.546 | -0.101 | -0.020 | 0.00 | 0.00 | 0.00 |
| 90.03 | 450.15 | 450.00 | 450.198 | 199.900 | 39960.186 | 89955.198 | -0.049 | -0.010 | -0.15 | -0.03 | -0.01 |
| 80.1 | 400.50 | 401.00 | 400.496 | 150.250 | 22575.042 | 60250.223 | 0.002 | 0.000 | 0.50 | 0.13 | 0.05 |
| 70 | 350.00 | 350.00 | 349.944 | 99.750 | 9949.975 | 34912.347 | 0.055 | 0.011 | 0.00 | 0.00 | 0.00 |
| 60 | 300.00 | 300.00 | 299.892 | 49.749 | 2474.997 | 14924.804 | 0.106 | 0.021 | 0.00 | 0.00 | 0.00 |
| 50.04 | 250.20 | 250.00 | 250.040 | -0.051 | 0.003 | -12.682 | 0.158 | 0.032 | -0.20 | -0.08 | -0.02 |
| 40.08 | 200.40 | 200.00 | 200.189 | -49.851 | 2485.088 | -9970.131 | 0.210 | 0.042 | -0.40 | -0.20 | -0.04 |
| 30.14 | 150.70 | 150.00 | 150.437 | -99.550 | 9910.290 | -14932.566 | 0.262 | 0.052 | -0.70 | -0.46 | -0.07 |
| 20.04 | 100.20 | 100.00 | 99.885 | -150.050 | 22515.025 | -15005.007 | 0.314 | 0.063 | -0.20 | -0.20 | -0.02 |
| 10.12 | 50.60 | 50.00 | 50.235 | -199.650 | 39859.951 | -9982.478 | 0.365 | 0.073 | -0.60 | -1.18 | -0.06 |
| 0 | 0.00 | 0.00 | -0.417 | -250.249 | 62624.515 | 0.000 | 0.417 | 0.083 | 0.00 | | 0.00 |
| Average | 250.25 | 250.09 | Sums (Σ) | 0.000 | 274730.680 | 275015.253 | | Average | -0.16 | -0.20 | -0.02 |
| | | | Slope | | B= | 1.001 | | Maximum | -0.70 | -1.18 | -0.07 |
| | | | Offset | | A= | -0.417 | | | | | |

EN14181 spec: dcrel <2%

Pass/Fail

PASS



Linearity Test Certificate



Signal Group Ltd
Standards House, Doman Road
Camberley, Surrey GU15 3DF UK
Tel: +44 (0)1276 682841
Fax: +44 (0)1276 691302
Web: www.signal-group.com

INSTRUMENTATION

| Instrument Details | Serial No. | Range FS |
|--------------------|------------|----------|
| 4000VM | 14951 | 1000 |

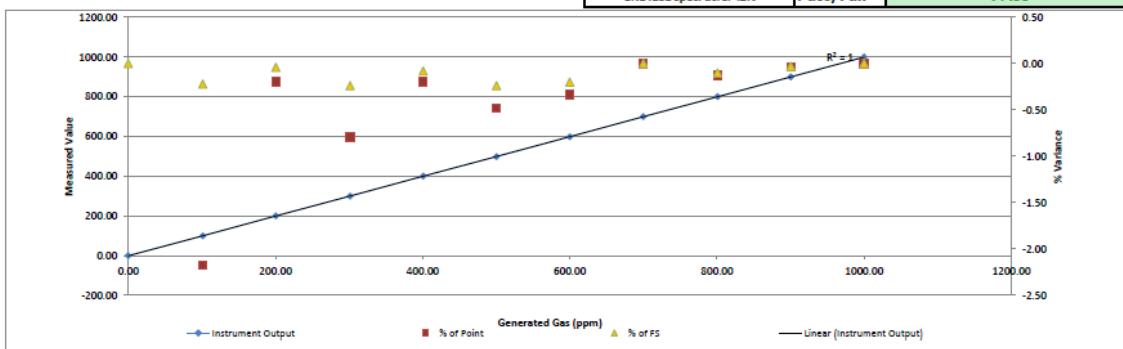
TRACEABILITY

| Gas Divider Details | Serial No. | Calibration Date |
|---------------------|------------|------------------|
| 821s | 9367 | 18.04.2023 |

| Analytical Traceability | | | |
|-------------------------|--------------|----------|-----------------|
| | Cylinder No. | Gas type | Gas value (ppm) |
| Span Gas | EA54AYA | NO | 1000 |
| Mixture | | | |
| Diluent gas | KN27XDK | N2 | |

LINEARITY

| Gas Divider Point | Actual | Measured | Regression fit | | | | | | Variance | | |
|-------------------------|---------|----------|----------------|----------|-------------|-------------|----------------|------------------|------------|----------------|-----------|
| | ppm | ppm | y | (c-c) | (c-c)^2 | x*(c-c) | d _c | d _{rel} | (ppm or %) | (% of reading) | (% of FS) |
| 100 | 1000.00 | 1000.00 | 999.385 | 499.504 | 249504.617 | 499504.372 | 0.615 | 0.062 | 0.00 | 0.00 | 0.00 |
| 90.03 | 900.30 | 900.00 | 899.597 | 399.802 | 159841.445 | 359821.582 | 0.700 | 0.070 | -0.30 | -0.03 | -0.03 |
| 80.1 | 801.00 | 800.00 | 800.210 | 300.500 | 90300.087 | 240399.783 | 0.786 | 0.079 | -1.00 | -0.12 | -0.10 |
| 70 | 699.99 | 700.00 | 699.123 | 199.498 | 39799.554 | 139648.779 | 0.871 | 0.087 | 0.01 | 0.00 | 0.00 |
| 60 | 599.99 | 598.00 | 599.037 | 99.497 | 9899.729 | 59499.434 | 0.958 | 0.096 | -1.99 | -0.33 | -0.20 |
| 50.04 | 500.39 | 498.00 | 499.352 | -0.103 | 0.011 | -51.249 | 1.043 | 0.104 | -2.39 | -0.48 | -0.24 |
| 40.08 | 400.79 | 400.00 | 399.667 | -99.703 | 9940.613 | -39881.049 | 1.127 | 0.113 | -0.79 | -0.20 | -0.08 |
| 30.14 | 301.39 | 299.00 | 300.183 | -199.102 | 39641.511 | -59531.427 | 1.213 | 0.121 | -2.39 | -0.79 | -0.24 |
| 20.04 | 200.40 | 200.00 | 199.098 | -300.100 | 90060.187 | -60020.059 | 1.297 | 0.130 | -0.40 | -0.20 | -0.04 |
| 10.12 | 101.20 | 99.00 | 99.816 | -399.298 | 159439.114 | -39530.529 | 1.383 | 0.138 | -2.20 | -2.17 | -0.22 |
| 0 | 0.00 | 0.00 | -1.468 | -500.496 | 250495.874 | 0.000 | 1.468 | 0.147 | 0.00 | | 0.00 |
| Average | 500.50 | 499.45 | Sums (Σ) | 0.000 | 1098922.743 | 1099859.636 | | Average | -1.04 | -0.43 | -0.11 |
| | | | Slope | | B= | 1.001 | | Maximum | -2.39 | -2.17 | -0.24 |
| | | | Offset | | A= | -1.468 | | | | | |
| EN14181 spec: dcrel <2% | | | | | | | | Pass/Fail | PASS | | |



Calibrated by: RC

Signed: [Signature]

Date: 10.07.2023

10PPM C3H8 Linearity Test Certificate

0



Signal Group Ltd
Standards House, Dorman Road
Camberley, Surrey GU15 3DF UK
Tel: +44 (0)1276 692841
Fax: +44 (0)1276 691302
Web: www.signal-group.com

INSTRUMENTATION

| Instrument Details | Serial No. | Range FS |
|--------------------|------------|----------|
| 3000HM | 16122 | 10 |

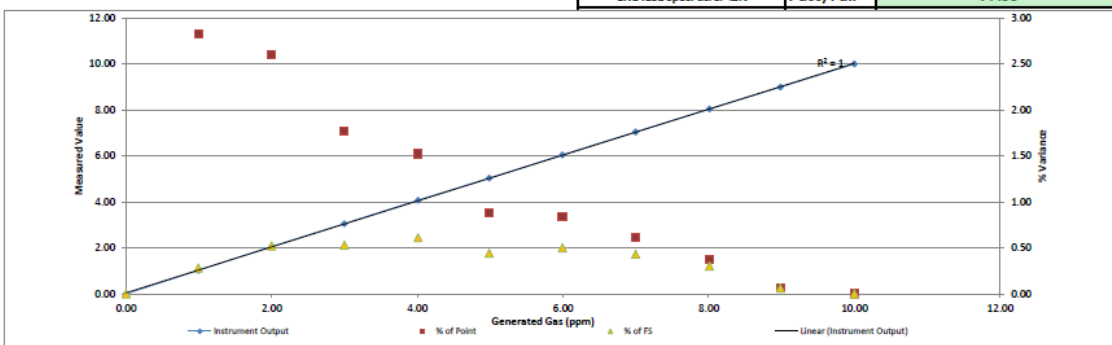
TRACEABILITY

| Gas Divider Details | Serial No. | Calibration Date |
|---------------------|------------|------------------|
| 821s | 12978 | 27/04/2023 |

| Analytical Traceability | | | |
|-------------------------|----------|-----------------|-------------|
| Cylinder No. | Gas type | Gas value (ppm) | Balance gas |
| HQ29 MQK | C3H8 | 10 | AIR |
| Span Gas Mixture | | | |
| Diluent gas | AIR | | |

LINEARITY

| Gas Divider Point | Actual | Measured | Regression fit | | | | | | | Variance | | |
|-------------------------|--------|----------|----------------|--------|--------------------|---------|----------------|------------------|---------|------------|----------------|-----------|
| | ppm | ppm | y | (c-c) | (c-c) ² | x*(c-c) | d _y | d _{rel} | | (ppm or %) | (% of reading) | (% of FS) |
| 100 | 10.00 | 10.00 | 10.025 | 5.003 | 25.034 | 50.034 | -0.025 | -0.250 | | 0.00 | 0.00 | 0.00 |
| 89.84 | 8.98 | 8.99 | 9.011 | 3.987 | 15.899 | 35.846 | -0.027 | -0.267 | | 0.01 | 0.07 | 0.06 |
| 80.1 | 8.01 | 8.04 | 8.038 | 3.013 | 9.080 | 24.227 | -0.028 | -0.283 | | 0.03 | 0.37 | 0.30 |
| 69.97 | 7.00 | 7.04 | 7.027 | 2.000 | 4.001 | 14.083 | -0.030 | -0.299 | | 0.04 | 0.61 | 0.43 |
| 59.9 | 5.99 | 6.04 | 6.022 | 0.993 | 0.987 | 6.000 | -0.032 | -0.316 | | 0.05 | 0.83 | 0.50 |
| 49.86 | 4.99 | 5.03 | 5.019 | -0.011 | 0.000 | -0.054 | -0.033 | -0.333 | | 0.04 | 0.88 | 0.44 |
| 40.09 | 4.01 | 4.07 | 4.044 | -0.988 | 0.975 | -4.020 | -0.035 | -0.349 | | 0.06 | 1.52 | 0.61 |
| 29.97 | 3.00 | 3.05 | 3.034 | -2.000 | 3.999 | -6.099 | -0.037 | -0.366 | | 0.05 | 1.77 | 0.53 |
| 19.98 | 2.00 | 2.05 | 2.036 | -2.999 | 8.992 | -6.147 | -0.038 | -0.383 | | 0.05 | 2.60 | 0.52 |
| 9.92 | 0.99 | 1.02 | 1.032 | -4.005 | 16.037 | -4.085 | -0.040 | -0.400 | | 0.03 | 2.82 | 0.28 |
| 0 | 0.00 | 0.00 | 0.042 | -4.997 | 24.966 | 0.000 | -0.042 | -0.418 | | 0.00 | | 0.00 |
| Average | 5.00 | 5.03 | Sums (Σ) | 0.000 | 109.971 | 109.786 | | | Average | 0.03 | 1.15 | 0.37 |
| | | | Slope | | B= | 0.998 | | | Maximum | 0.06 | 2.82 | 0.61 |
| | | | Offset | | A= | 0.042 | | | | | | |
| EN14181 spec: dcrel <2% | | | | | | | | | | Pass/Fail | PASS | |



100PPM C3H8 Linearity Test Certificate



Signal Group Ltd
Standards House, Doman Road
Camberley, Surrey GU15 3DF UK
Tel: +44 (0)1276 682841
Fax: +44 (0)1276 681302
Web: www.signal-group.com

INSTRUMENTATION

| Instrument Details | Serial No. | Range FS |
|--------------------|------------|----------|
| 3000HM | 16122 | 100 |

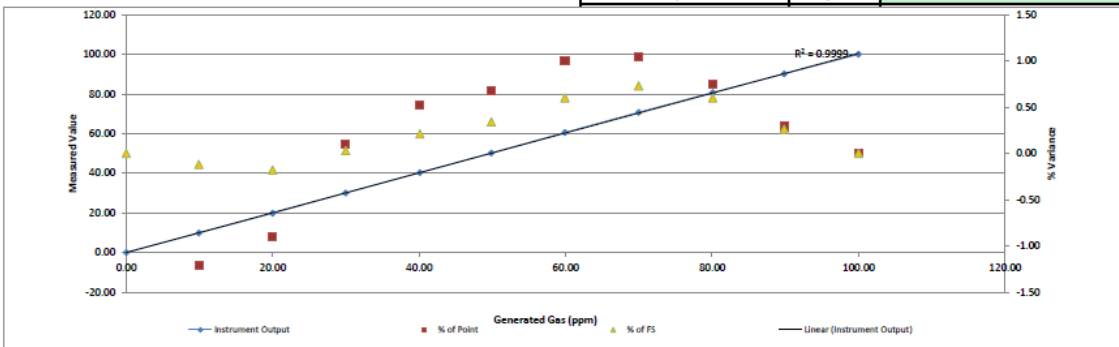
TRACEABILITY

| Gas Divider Details | Serial No. | Calibration Date |
|---------------------|------------|------------------|
| 821s | 12978 | 27/04/2023 |

| Analytical Traceability | | | |
|-------------------------|----------|-----------------|-------------|
| Cylinder No. | Gas type | Gas value (ppm) | Balance gas |
| EM41 QF8 | C3H8 | 100 | AIR |
| Span Gas Mixture | | | |
| Diluent gas | AIR | | |

LINEARITY

| Gas Divider Point | Actual | Measured | Regression fit | | | | | | | Variance | | |
|-------------------------|--------|----------|----------------|---------|--------------------|-----------|----------------|------------------|---------|------------|----------------|-----------|
| | ppm | ppm | y | (c-c) | (c-c) ² | x*(c-c) | d _c | d _{rel} | | (ppm or %) | (% of reading) | (% of FS) |
| 100 | 100.00 | 100.00 | 100.482 | 50.034 | 2503.365 | 5003.364 | -0.482 | -0.482 | | 0.00 | 0.00 | 0.00 |
| 89.84 | 89.84 | 90.10 | 90.269 | 39.874 | 1589.907 | 3592.615 | -0.431 | -0.431 | | 0.26 | 0.29 | 0.26 |
| 80.1 | 80.10 | 80.70 | 80.479 | 30.134 | 908.036 | 2431.784 | -0.382 | -0.382 | | 0.60 | 0.75 | 0.60 |
| 69.97 | 69.97 | 70.70 | 70.297 | 20.004 | 400.145 | 1414.257 | -0.331 | -0.331 | | 0.73 | 1.04 | 0.73 |
| 59.9 | 59.90 | 60.50 | 60.176 | 9.934 | 98.677 | 600.985 | -0.279 | -0.279 | | 0.60 | 1.00 | 0.60 |
| 49.86 | 49.86 | 50.20 | 50.084 | -0.106 | 0.011 | -5.339 | -0.226 | -0.226 | | 0.34 | 0.68 | 0.34 |
| 40.09 | 40.09 | 40.30 | 40.264 | -9.876 | 97.543 | -398.017 | -0.175 | -0.175 | | 0.21 | 0.52 | 0.21 |
| 29.97 | 29.97 | 30.00 | 30.092 | -19.996 | 399.855 | -599.891 | -0.122 | -0.122 | | 0.03 | 0.10 | 0.03 |
| 19.98 | 19.98 | 19.80 | 20.050 | -29.986 | 899.182 | -593.730 | -0.070 | -0.070 | | -0.18 | -0.90 | -0.18 |
| 9.92 | 9.92 | 9.80 | 9.939 | -40.046 | 1603.711 | -392.454 | -0.018 | -0.018 | | -0.12 | -1.21 | -0.12 |
| 0 | 0.00 | 0.00 | -0.032 | -49.966 | 2496.637 | 0.000 | 0.032 | 0.032 | | 0.00 | | 0.00 |
| Average | 49.97 | 50.19 | Sums (Σ) | 0.000 | 10997.069 | 11053.573 | | | Average | 0.22 | 0.23 | 0.25 |
| | | | Slope | | B= | 1.005 | | | Maximum | 0.73 | -1.21 | 0.73 |
| | | | Offset | | A= | -0.032 | | | | | | |
| EN14181 spec: dcrel <2% | | | | | | | | | | Pass/Fail | PASS | |



Calibrated by: A Cherry Signed: AC Date: 07/07/2023

Rosemount CO2 low:

WO:

Gas Type: CO2
Channel Range: 10000
Conc Units: ppm

| Linearizer DISABLED | | |
|---------------------|-----------------------------|----------------------|
| Setpoint | Actual Gas Divider Setpoint | Unlinearized Reading |
| 0 | 0 | 0 |
| 1000 | 1144 | 1923 |
| 2000 | 2214 | 3268 |
| 3000 | 3118 | 4306 |
| 4000 | 4095 | 5278 |
| 5000 | 5242 | 6355 |
| 6000 | 6057 | 7070 |
| 7000 | 7179 | 7985 |
| 8000 | 8086 | 8688 |
| 9000 | 9143 | 9440 |
| 10000 | 10050 | 10050 |

| Linearizer ENABLED | | | |
|----------------------|--------------------|-------------|------|
| Gas Divider Setpoint | Linearized Reading | Error (ppm) | %FS |
| 0 | 0 | 0.0 | 0.00 |
| 1144 | 1168 | 24.0 | 0.24 |
| 2214 | 2244 | 30.0 | 0.30 |
| 3118 | 3133 | 15.0 | 0.15 |
| 4095 | 4114 | 19.0 | 0.19 |
| 5242 | 5275 | 33.0 | 0.33 |
| 6057 | 6099 | 42.0 | 0.42 |
| 7179 | 7209 | 30.0 | 0.30 |
| 8086 | 8130 | 44.0 | 0.44 |
| 9143 | 9173 | 30.0 | 0.30 |
| 10050 | 10050 | 0.0 | 0.00 |
| 0 | | 0.0 | 0.00 |

Mark Torrance

| | |
|----------------|-----|
| Gas Type: | CO2 |
| Channel Range: | 10 |
| Conc Units | % |

| Linearizer DISABLED | | |
|---------------------|-----------------------------|----------------------|
| Setpoint | Actual Gas Divider Setpoint | Unlinearized Reading |
| 0 | 0 | 0 |
| 1 | 1 | 1.4 |
| 2 | 2 | 2.6 |
| 3 | 3 | 3.7 |
| 4 | 4 | 4.7 |
| 5 | 5 | 5.6 |
| 6 | 6 | 6.6 |
| 7 | 7 | 7.5 |
| 8 | 8 | 8.3 |
| 9 | 9 | 9.1 |
| 10 | 10 | 9.99 |
| | | |

| Linearizer ENABLED | | | |
|----------------------|--------------------|-------------|------|
| Gas Divider Setpoint | Linearized Reading | Error (ppm) | %FS |
| 0 | 0 | 0.0 | 0.00 |
| 1 | 1 | 0.0 | 0.00 |
| 2 | 2.1 | 0.1 | 1.00 |
| 3 | 3 | 0.0 | 0.00 |
| 4 | 4 | 0.0 | 0.00 |
| 5 | 5 | 0.0 | 0.00 |
| 6 | 6 | 0.0 | 0.00 |
| 7 | 7 | 0.0 | 0.00 |
| 8 | 8 | 0.0 | 0.00 |
| 9 | 9 | 0.0 | 0.00 |
| 10 | 10 | 0.0 | 0.00 |
| | | | |

Mark Torrance

[illegible]



European Union Aviation Safety Agency

Konrad-Adenauer-Ufer 3
50668 Cologne
Germany

[Environmental Research - Engine Emissions | EASA](#)

Mail EASA.research@easa.europa.eu
Web www.easa.europa.eu

An Agency of the European Union

